Sulfur-cycling and microorganisms of the Frasassi cave system, Italy

By: Danielle Eastman
Research Advisor: Dr. Gregory Druschel

Senior Thesis 2007
University of Vermont
Burlington VT, 05401

In Collaboration with:
Dr. Jenn Macalady
Dan Jones
Lindsey Albertson

Penn State University
State College, PA

Abstract

Sulfur utilizing bacteria in the Frasassi cave system of central Italy significantly contribute to the sulfur chemistry of the system. Microbial communities of sulfur-reducing and sulfur-oxidizing organisms in the sub-aqueous regions of the caves, as well as on the walls and ceilings, are catalysts for the majority of the oxidation-reduction reactions involved in sulfur cycling. Sulfide oxidation is the primary reaction of these chemical systems and fuels sulfuric acid speleogenesis. The overall rate at which sulfide is oxidized is dictated by biotic oxidation, which occurs at a much faster rate than abiotic oxidation. The sulfuric acid produced through biotic sulfide oxidation represents a biologically mediated process of speleogenesis.

In addition to hosting a diverse selection of sulfur bacteria, including *Beggiatoa spp, Thiovulum,* and δ-proteobacteria, these sulfidic caves served as a natural laboratory for investigating the link between sulfur chemistry and biology. For this thesis a variety of chemotrophic microbial ecosystems, as well as phototrophic sulfur bacteria of the Frasassi caves, were studied. The comparison of these microbial communities provided information defining the pathways through which sulfur is oxidized, the rate at which oxidation occurs, and the chemical parameters that select for the dominant bacterial species of that community.

Chemical niches, which selected for and are influenced by the bacteria, were investigated using electrochemical techniques. Specifically, voltammetry was used to detect intermediate species of sulfur over space and time. *In situ,* real-time measurements using Au/Hg amalgam solid-state glass electrodes yielded details of chemical cycling through microbial biofilms, water columns, and sediment. Voltammetry provided detailed measurements and allowed for comparisons of different microbial ecosystems in the caves. The intermediate species of sulfur detected in these ecosystems and changes in the chemistry over time and space have implications for the rate of sulfide oxidation and the pathways through which sulfide is oxidized. If we can better understand these pathways we can better determine the rate of oxidation and how different environmental conditions select for different populations of microorganisms.

Table of Contents

Page

1.0 Introduction 5

1.1 Project Objectives 5

1.2 Geological History Frasassi 6

1.3 Cave Formation 7

1.4 Sulfur Bacteria 11

1.4.1 Background on Sulfur Bacteria 11

1.4.2 Sulfur bacteria observed at Frasassi 13

1.5 Sulfur Chemistry 16

1.5.1 Intermediate Sulfur Species 16

1.5.2 Biotic Sulfur Oxidation 19

1.5.2.1 Chemotrophic Oxidation 19

1.5.2.2 Phototrophic Oxidation 21

1.5.3 Rates of Sulfide Oxidation 23

2.0 Methods 28

2.1 Analytical Instruments 28

2.1.1 Electrochemical Analysis: Voltammetry 28

2.1.2 Colorimetery and pH measurements 30

2.1.3 Raman Spectroscopy 30

2.2 Field Methods 31

2.2.1 Vertical and Horizontal Spatial analysis of biofilm mats 31

2.2.2 Temporal Analysis 31

2.2.3 Light Manipulation Experiments 32

2.3 Lab experiments 32

2.3.1 Standards 32

2.3.2 Testing of electrodes 33

2.3.3 Identification of sulfur species in Cave Spring water 34

2.3.4 Elemental sulfur solubility experiments 35

3.0 Results 37

3.1 Lab Experiments 37

3.1.1 Elemental Sulfur: Colloidal vs. Dissolved 40

3.1.2 Sulfide Calibration 40

3.1.3 Polysulfide vs. Sulfide 40

3.2 Field Data 42

3.2.1 Cave Spring 42

3.2.2 Lago Verdi 44

3.2.3 Grotto Sulfureo 45

3.2.4 Ramo Sulfureo 46

3.2.5 Pozzo di Cristali 49

3.2.5.1 Observations 49

3.2.5.2 Lateral Spatial Analysis 49

3.2.5.3 Vertical profile 52

3.2.5.4 Rates of Oxidation at Pozzo di Cristali 54

3.2.6 Phototrophic Bacteria 56

3.2.6.1 Cyanobacteria: Fissure Spring 56

3.2.6.2 Purple Sulfur Bacteria 58
4.0 Discussion 60
4.1 Elemental Sulfur Solubility 60
4.2 Microbial communities of the Frasassi cave system and their chemical niches 62
4.2.1 Feathery Biofilm 62
4.2.2 Thin White Biofilm 62
4.2.3 Phototrophic Biofilm 63
4.3 Defining chemical niches based on intermediate sulfur chemistry 64
4.4 Rates of sulfide oxidation and its significance to cave formation: Pozzo di Cristali 66
5.0 Conclusion 68
6.0 Future Work 69
Literature Cited 70

1.0 Introduction

1.1 Project Objectives

The Frasassi cave system is a rare natural setting for studying sulfur-utilizing bacteria. It is a simple environment with chemical systems dominated by sulfur. The caves are also the same temperature year round and there is a lack of sunlight. The relative simplicity of the cave environment allows us to study its chemical systems in more detail by eliminating many variables found in other natural environments. This facilitates investigation of the core processes between microbes and sulfur cycling. If we can better understand the pathways through which sulfur is oxidized, we can better determine the rate of oxidation and how different environmental conditions select for different populations of microorganisms.

The Frasassi cave system supports an array of biology, ranging from microbial biofilm mats to insects and gastropods to bats and eels. The chemistry becomes more complex in deeper sections of the cave system with the presence of stratified lakes. This research, however, focuses on microbial communities dominating streams and small lakes inside shallow sections of the cave, as well as the microbiology at two cave spring exits. Several sites of the Frasassi cave system were studied in an effort to understand the variety of microbial ecosystems and their associated chemistries. Phototrophic biofilm mats were also studied in the Sentino River which runs through the Frasassi Gorge, adjacent to the cave springs.

The investigation of sulfur cycling is important in determining the redox conditions in a variety of chemical systems. The effects of microbes on these conditions are a significant part of studying the system. It is important to understand what microbes

do in any environment and exactly how they are affected by environmental changes. Sulfur cycling is central to various environments worldwide and is significant for soil fertilization, transportation of nutrients, mobilization of metals and organic contaminants in wetlands and aquifers (Teske and Nelson, 2006). Understanding the role of specific microbial species in different environments and geochemical conditions could be applied to a variety of geochemical problems where microbes are key components of chemical cycling, such as contaminant remediation through bio-stimulation/biocogmentation.

1.2 Geological History Frasassi

The Frasassi cave system is located in the Calcare Massiccio formation of the Umbria-Marche region in central Italy. The Calcare Massiccio limestone dates back to the Jurassic Era, which is characterized by wide spread shallow ocean basins (Montanari et al., 2002). This depositional environment was similar to the carbonate platforms forming in the Bahamas today. In the area which is now the Umbria-Marche region, these shallow marine environments produced the 600 to 800 meter thick Calcare Massiccio limestone (Montanari et al., 2002). The Calcare Massiccio limestone is comprised of thick depositional beds and a homogeneous composition of fine-grained calcium carbonate (Montanari et al., 2002).

The deposition and lithification of the Calcare Massiccio was followed by several periods of extension, lasting from 100 to 50 Ma. This extension was caused by the rifting of the European and African plates (Montanari et al., 2002). These periods of extension resulted in the formation of a network of normal faults producing a horst and graben topography in the newly formed ocean basin. In association with the tectonic activity, turbidites and mega-breccias formed and are interbedded in much of the sedimentary

deposits of the region (Montanari et al., 2002). During tectonic quiescence, finer grained calcareous sediment was deposited on the ocean basin (Montanari et al., 2002).

In the Miocene Epoch the tectonic regime shifted from extension to compression with the convergence of the African and European plates. Compression reactivated normal fault zones associated with prior rifting events. This reactivation created reverse faults and sparked the orogeny of the Apennine Mountains. The deformation associated with plate compression and subsequent uplift of the sedimentary basins resulted in a series of anticlinal and synclinal folds.

1.3 Cave Formation

The landscape and geology of the Frasassi region, an area which is still tectonically active, reflects millions of years of tectonism, weathering, and erosion. As the Sentino River eroded through the sedimentary cover of the region and tectonic uplift changed the topography, the Frasassi cave system recorded these changes. There are several stages of karst formation which correspond with uplift of the Apennine Mountains. Three main uplift events are recorded in the cave system as three separate levels (figure 1.1). Each level was formed from a combination of tectonic uplift and erosion by the Sentino River and represents a period of time during which the groundwater interacted with that part of the limestone (Montanari et al., 2002). The bottom-most level to the Frasassi cave system is the youngest and is currently being further developed (figure 1.1) (Montanari et al., 2002).

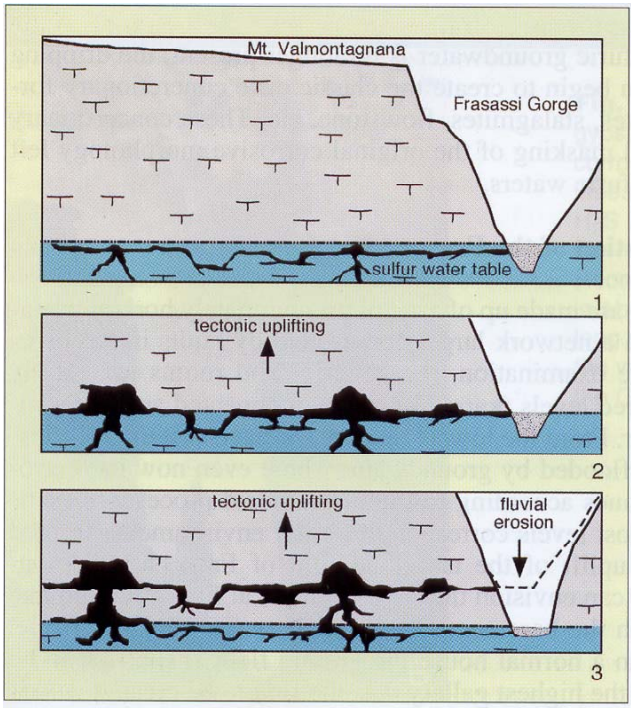

Figure 1.1: The progressive sequence of uplift and cave formation of the Frasassi cave system. (From Montanari et al., 2002)

Most limestone karst systems, including the Frasassi cave system, form through the interaction of carbonic acid with calcium carbonate. Carbon dioxide in the atmosphere reacts with water forming carbonic acid (equation 1.1). Carbonic acid then reacts with calcium carbonate in a dissociation reaction, producing bicarbonate and releasing calcium ions into solution (equation 1.2).

$$CO_2 + H_2O = H_2CO_3 \quad (1.1)$$

$$CaCO_{3(s)} + H_2CO_3 = Ca^{2+} + 2HCO_3^- \quad (1.2)$$

In the specific case of the Frasassi caves, sulfuric acid is being generated in addition to carbonic acid. Sulfuric acid is a stronger acid than carbonic acid and accelerates cave formation by the dominant process referred to as *sulfuric acid speleogenesis* (Vlasceanu et al., 2000). Sulfidic waters run through the Frasassi caves, creating a chemical system defined by sulfur cycling and sulfur utilizing bacteria. The

Frasassi caves are among only a small number of caves in the world that are forming through sulfuric acid speleogenesis, including Lower Cane Cave (Wyoming), Movile Cave (Romania), Parker Cave (Kentucky), and Cesspool Cave (Virginia) (Macalady et al., 2006). The following mat shows the network of caves that makes up the Frasassi cave system, as explored to date:

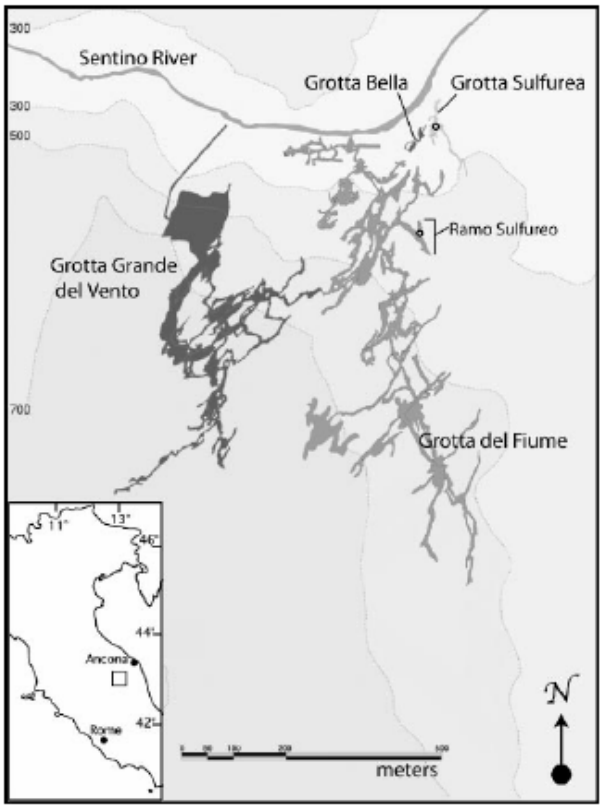

Figure 1.2: Map of the Frasassi cave system, Italy with topographic contour for reference. (Adapted from Macalady et al., 2006)

The origin of the sulfidic groundwater feeding the Frasassi cave system is not completely understood. There are two theories which include the dissolution and reduction of deep sulfate mineral deposits, such as gypsum and anhydrite, during the transport of the water into the Calcare Massicio limestone. In both scenarios, sulfate is dissolved into the groundwater and interacts with organics associated with the rock formations. One theory suggests that groundwater passes through the Burrano Formation, which is stratigraphically lower and older than the Calcare Massicio limestone (Montanari et al., 2002). The second theory suggests that the Gessoso-Solfifera Formation is the source for the sulfidic groundwater (Montanari et al, 2005). As a result of thrust-faulting during Miocene compressional events, the younger, sulfate-rich Gessoso-Solfifera Formation is stratigraphically lower than the Calcare Massicio.

The waters which pass through the caves are not rich in sulfate; rather they are rich in sulfide. Microbial activity may be responsible for creating a reducing environment at depth, using energy from the interaction between sulfate and organics, reducing the sulfate to sulfide in the deep groundwater. As the deep sulfidic groundwater moves to the surface, it interacts with oxic meteoric water and atmospheric oxygen, creating a redox gradient between oxygen and sulfide (Montanari et al., 2002). The oxidation of sulfide proceeds in many steps and is mediated by microbial communities of sulfur bacteria which occupy narrow zones within the redox gradient (Teske and Nelson, 2006). Sulfuric acid forms as a byproduct of the biotic and abiotic oxidation of sulfide and is the main component in speleogenesis of the Frasassi cave system. Equations 1.3 and 1.4 explain the formation of sulfuric acid and its reaction with calcite (Macalady et al., 2006).

$$H_2S + 2O_2 = H_2SO_4 \quad (1.3)$$

$$CaCO_3 + H_2SO_4 = Ca^{2+} + SO_4^{2-} + HCO_3^- + H^+ \quad (1.4)$$

Aqueous regions of the caves are most effective at corroding the limestone. Macalady et al., 2005 estimate that 15mg $CaCO_3$ per cm^2 of limestone is corroded away each year. The enormous size of the caves in relation to the amount of water passing through them, as well as the bowl shape of many of these rooms, suggests that the rate of speleogenesis is accelerated in aqueous regions of the caves. Several factors contribute to the efficiency of speleogenesis in aqueous regions. Microbial communities, which occupy redox gradients in the water column, are known to mediate sulfide oxidation and the resulting sulfuric acid production. These regions provide a large source of sulfide and inhabit microbial communities of sulfur bacteria which accelerate oxidation reactions (Hagen and Nelson, 1997).

Gypsum on the walls and ceilings of the caves records sulfuric acid speleogenesis over time (Vlasceanu, 2000). Gypsum ($CaSO_4$) is an evaporite mineral and forms from calcium and sulfate ions, which are products of the reaction between calcite and sulfuric acid (equation 1.4). Therefore, gypsum is specifically indicative of sulfuric acid speleogenesis.

1.4 Sulfur Bacteria

1.4.1 Background on Sulfur Bacteria

Sulfur bacteria are phylogenetically deep branching organisms which utilize the energy associated with sulfur reduction and oxidation for metabolic energy, cell maintenance, and growth. They are found in sulfide-rich environments, including

geothermal springs, oceanic geothermal vents, sulfidic cave systems, and sulfide-rich industrial sites (Teske and Nelson, 2006). The chemical and physical conditions of an environment will select specific species of microbes in a community. The efficiency with which certain species of bacteria can harness energy from a chemical system, as well as contribute to the efficiency of the microbial community as a whole, will determine the dominant species in that microbial community.

Sulfur oxidizing bacteria are classified based on their shape, size, techniques for oxidation, and features helpful for environmental adaptation. The ability to adapt to changes in the environment is a significant advantage for bacteria. This adaptation can happen in two ways: through ecological flexibility and plasticity (Canfield et al., 2005). Ecological flexibility refers to the adaptation of the entire microbial community in response to environmental changes. For example, a change in the amount of oxygen in the environment might trigger an ecological shift in the microbial community to one which is dominated by organisms that can survive in the oxic conditions (Canfield et al., 2005).

Plasticity is similar to ecological flexibility but it describes adaptation techniques specific to each species. There are a number of ways in which individual species have evolved to adapt to environmental changes. Flagellum, which is an appendage capable of rotation and enables cell mobility, is an example of an adaptation apparatus characteristic of many sulfur oxidizing bacteria, such as *Beggiatoa spp* (Madigan et al., 2002).

Several species of sulfur bacteria, both oxidizers and reducers, are often incorporated into complex biofilm mats. For example, although *Beggiatoa spp* lack photosynthetic pigments, they are often associated with cyanobacterial mats. As the

cyanobacteria utilize photosynthetic energy during the day, the top part of the mat becomes supersaturated with oxygen (Teske and Nelson, 2006). At night oxygen production ceases, and sulfate reduction from the bottom of the mat becomes the dominant source of energy (Teske and Nelson, 2006). This daily process creates a vertically fluctuating gradient of oxygen and sulfide. *Beggiatoa spp* are able to move vertically with this gradient with a gliding speed of 1 to 2.6 μm per second (Teske and Nelson, 2006). In doing so they are able to stay within the location where sulfide and oxygen coexist, oxidizing the sulfide and contributing to chemical cycling through the mat (Teske and Nelson, 2006). They are also able to use the cyanobacterial mat as a form of protection from sunlight, thus maintaining a safe position in the mat (Teske and Nelson, 2006).

1.4.2 Sulfur bacteria observed at Frasassi

Autotrophic, heterotrophic, phototrophic, and acidophilic species of sulfur bacteria inhabit the Frasassi cave system, making Frasassi an excellent natural laboratory for studying sulfur cycling through a variety of microbial ecosystems. The phylogenetic diversity of the biofilm mats suggests complex sulfur cycling through microbial ecosystems (Macalady et al., 2005). Microbial communities of sulfur-reducing and sulfur-oxidizing organisms in the aqueous regions of the Frasassi caves, as well as on the walls and ceilings, are catalysts for the majority of the oxidation-reduction reactions involved in sulfur cycling through the caves. These reactions are fueling sulfuric acid production and represent a biologically mediated process of speleogenesis (Macalady et al, 2005).

A summary of the main characteristics of various species of sulfur bacteria found in the Frasassi caves is presented in Table 1. Macalady et al, 2005 categorized the microbial communities of Frasassi into two groups, "cottony" and "feathery", based on their physical appearance. The cottony classification describes thin white mats dominated by *Beggiatoa spp*-like filaments intertwined with δ-proteobacteria as well as *Thiovulum* (Macalady et al., 2005). The feathery mats were much thicker and were associated with faster flowing waters. These mats were dominated by *Thiothrix*-like δ-proteobacteria, and ε-proteobacteria filaments (Macalady et al., 2005).

The walls of the caves also hosted microbial activity. A zebra-like pattern created by microbial communities decorated the surfaces of many cave walls and *Snottites* (figure 1.3) hung from the surface of gypsum crystals. These Snottites were very acidic, with a pH of around three and were the only wall biofilms studied because of equipment restrictions.

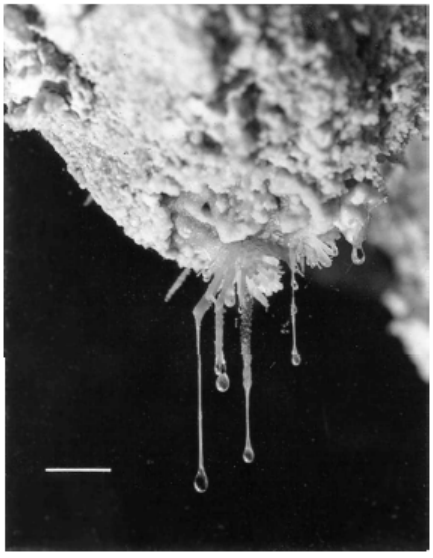

Figure 1.3: Picture of snottites hanging from gypsum crystals on the walls of the Frasassi cave. (Vlasceanu, 2000) Scale is 2cm

For this thesis phototrophic sulfur oxidizing organisms were also studied at Frasassi, just outside the caves in the Sentino River. A cyanobacteria mat and a purple sulfur bacteria mat were studied in 2005 and 2006. Although cyanobacteria and purple sulfur bacteria are relatively well known organisms, the mats specific to Frasassi are not well understood. It is anticipated that genomic and chemical analysis of the mats will yield valuable information for understanding sulfur cycling, in association with photosynthesis (Macalady et al., in prep).

Beggiatoa spp:	- Autotrophic and heterotrophic - Can use both O_2 and NO_3^- - δ-proteobacteria - Characterized by filamentous morphology and storage of sulfur globules. - *Beggiatoa spp* thrive in environments with steep oxygen and sulfide gradients.
Thiothrix	- Autotrophic and heterotrophic - δ-proteobacteria - Filamentous - Like O_2 for electron acceptor - Occupy H_2S/O_2 interface
Thiovulum	- Autotrophic - ε-proteobacteria - Use O_2 as an electron acceptor - Highly mobile - Create veil for adaptation strategy
Cyanobacteria	- Phototrophic bacteria - Incorporate sulfide-oxidizing bacteria into mat - Can reduce sulfur in absence of oxygen
Purple Sulfur Bacteria	- γ-proteobacteria - Phototrophic - Light pigments complex determines niche (Example: Bchl a and Bchl b) - Mobile

Table 1: Main characteristics of sulfur bacteria found in Frasassi, as well as related species. (Canfield et al., 2005; Madigan et al., 2002; Macalady et al., 2005)

1.5 Sulfur Chemistry

1.5.1 Intermediate Sulfur Species

The oxidation reaction of sulfide to sulfate (equation 5) is a reaction involving eight electrons and proceeds in many steps. Sulfide (S^{2-}) is the most reduced form of sulfur and sulfate (SO_4^{-2}) is the most oxidized form (figure 1.4). Intermediate compounds of sulfur are formed during the oxidation process and include elemental sulfur (equation 1.6), thiosulfate (equation 1.7), sulfite (equation 1.8), and polysulfide (equation 1.9) (Steudel, 1986; Lorenson, 2005) (figure 1.4). The stability of the intermediates depends on pH, temperature, oxidizing agents, catalysts, and the composition of species in solution (Knickerbocker et al., 2000). The formation of different sulfur compounds can occur through abiotic and biotic oxidation of reduced sulfur species (Amend et al., 2003). The most common reduced sulfur compounds utilized by sulfur oxidizing bacteria are sulfide (H_2S), elemental sulfur (S^0), and thiosulfate ($S_2O_3^{2-}$).

$$HS^- + 2O_2 \rightarrow SO_4^{2-} + H^+ \quad (1.5)$$
$$HS^- + \tfrac{1}{2}O_2 \rightarrow S^0 + OH^- \quad (1.6)$$
$$HS^- + O_2 \rightarrow \tfrac{1}{2}\, S_2O_3^{2-} + \tfrac{1}{2}H_2O \quad (1.7)$$
$$HS^- + {}^2/_3O_2 \rightarrow SO_3^{2-} + H^+ \quad (1.8)$$
$$S_n + HS^- + OH^- \rightarrow S_{n+1}^{2-} + H_2O \quad (1.9)$$

Figure 1.4 Intermediate species of sulfur and their associated oxidation state. (Adopted from Williamson and Rimstidt, 1992)

The first product of sulfide oxidation is elemental sulfur, which exists as two states: dissolved and colloidal (Steudel & Holdt, 1988; Kleinjan et al, 2005). Colloidal sulfur is observed in aqueous environments suspended in the water as a function of its small size and hydrophobicity. The colloidal sulfur can be produced by acidification of polysulfide and thiosulfate to a pH around two (Wang et al., 1998). Acidified polysulfide and thiosulfate solutions will turn a milky-white color upon the formation of elemental sulfur. In natural environments organic polymers may adsorb to colloidal particles, altering their solubility by making them more hydrophilic (Kleinjan et al., 2003). Kleinjan et al. (2005) were able to distinguish between the two particles of sulfur as a function of their size (figure 1.5). They discovered that particle size has implications for the mobility of sulfur in an environment, its availability for biooxidation, and its significance to the kinetics of polysulfide and hydrogen sulfide formation (Kleinjan et al., 2005).

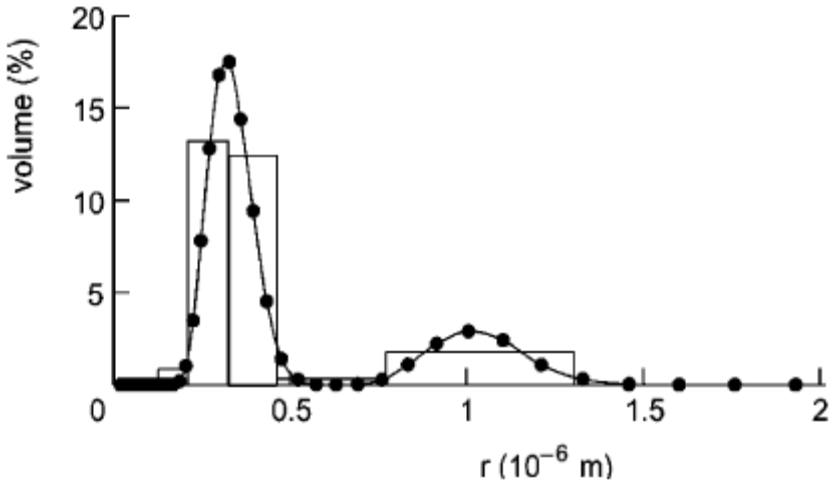

Figure 1.5: Elemental sulfur particle sizes after filtration with 3-µm filter. Adapted from Kleinjan et al. (2005)

Dissolved sulfur can be produced biotically and abiotically (Amend et al., 2003). Biosulfur is generated through biotic oxidation of sulfide and can be stored intercellularly or extracellularly in the form of sulfur globules (Kleinjan et al., 2003). Organic end groups and absorbed organic polymers, such as proteins, are responsible for biosulfur's hydrophilic characteristic (Kleinjan et al., 2003). The characteristics of biosulfur may differ between species of sulfur bacteria (Kleinjan et al., 2003). For example, phototrophic microorganisms are responsible for the production of structurally different biosulfur globules than chemotrophic bacteria (Kleinjan et al., 2003). Phototrophic bacteria produce long sulfur chains stabilized by organics; whereas chemotropic bacteria generate sulfur rings consisting of eight sulfur atoms (Kleinjan et al., 2003).

Steudel and Holdt (1988) found that organic surfactants, such as sodium dodeclysulfate (SDS), solubilize the colloidal sulfur and are thought to mimic natural organics. Solubility of elemental sulfur in water was found to be 5ug/L at 20ºC by a set of experiments conducted by Steudel et al. (1988). In their experiments they found elemental sulfur to be at least 5000 times more soluble in the presence of a neutral

surfactant. By following the solubility techniques used by Steudel and Holdt (1988), Loreson et al. (2006) was able to detect colloidal sulfur particles using voltammetry. In addition to detecting colloidal sulfur (electrical potential at -0.9 V), dissolved sulfur was identified at a peak potential of -1.2 V. Lorenson et al. (2006) was able to filter out one of the two peaks associated with elemental sulfur by using a 0.45-µm filter, showing the size dependence of the two signals.

1.5.2 Biotic Sulfur Oxidation

1.5.2.1Chemotrophic sulfide oxidation

Microorganisms will utilize the energy associated with combining oxidized and reduced species along redox gradients and further catalyze the redox reactions through various pathways (Knickerbocker et al., 2000). Microbes use the energy gained through these reactions to fixate CO_2 and facilitate cellular metabolism (Knickerbocker et al, 2000). Various species of sulfur bacteria have specific pathways for oxidizing or reducing sulfur compounds. In sulfidic environments many intermediate sulfur compounds can be present as a result of the biotic and abiotic redox reactions between sulfide and sulfate. Different oxidation and metabolic pathways will dictate the intermediate compounds produced and utilized by specific organisms (Kleinjan et al., 2003).

Communities of microbes may colonize together to take advantage of the energy associated with the intermediate sulfur compounds (equations 1.5-1.9). The species composition of a microbial community selects for the type of reduced sulfur compounds oxidized and the intermediate sulfur compounds produced. The initial step in biotic

sulfide oxidation is the oxidation of sulfide to (H_2S) to elemental sulfur (S^0) or sulfite (SO_3^{2-}) (Canfield et al, 2005). The elemental sulfur is often stored in cellular material by the organisms and can be used for further oxidation to sulfite during times of low sulfide conditions (Kleinjan et al., 2003). It is unusual for elemental sulfur to exist in aqueous environments because crystalline elemental sulfur is hydrophobic. The ability to solubilize elemental sulfur is a distinct characteristic of many sulfur bacteria, including *Beggiatoa spp*. Elemental sulfur can be stored by bacteria in the form of sulfur globules and can exist either intracellularly or extracellularly.

In addition to elemental sulfur this initial step of sulfide oxidation can also form polysulfide using *c*-type cytochromes (Canfield et al., 2005). A "reverse" siroheme-containing sulfite reducase is responsible for oxidizing polysulfide and elemental sulfur to sulfite, as well as the direct oxidation of sulfide to sulfite (Canfield et al, 2005). Many species of sulfur oxidizing bacteria oxidize thiosulfate ($S_2O_3^{2-}$), which is split into S^0 and SO_3^{2-} and can be further oxidized to sulfate (SO_4^{2-}). Sulfite is produced through various pathways and is a common product of biotic sulfur oxidation (Canfield et al, 2005). Sulfite is eventually oxidized to sulfate, unless it is utilized by sulfite reducing bacteria.

Electrons involved in the oxidation of reduced sulfur compounds are harnessed in the electron transport system of the bacterial cell. The transport of the electrons generates a proton motive force, which leads to adenosine triphosphate (ATP) synthesis by the enzyme ATPase. ATP is a high-energy compound responsible for supplying cellular energy (Madigan et al., 2002). Reverse electron flow yields NADH, a reducing compound used to fix CO_2 for cell maintenance, growth, and metabolism (Madigan et al., 2002).

Certain species of sulfur bacteria are able to use nitrate as an electron acceptor in the absence of oxygen (Kamp et al, 2006). In anaerobic environments species of sulfur bacteria can not only exist, but thrive using nitrate instead of oxygen (Kamp et al, 2006). The following reactions show the microbial oxidation of sulfide using oxygen (equations 1.10 and 1.11) and nitrate (equations 1.12 and 1.13) (Teske and Nelson, 2006).

$$H_2S + 2O_2 \rightarrow H_2SO_4 \quad (1.10)$$
$$2H_2S + O_2 \rightarrow 2S^0 + 2H_2O \quad (1.11)$$
$$5H_2S + 8NO_3^- \rightarrow 4N_2 + 5SO_4^{2-} + 2H^+ + 4H_2O \quad (1.12)$$
$$H_2O + NO_3^- + H_2O \rightarrow SO_4^{2-} + NH_4^+ \quad (1.13)$$

1.5.2.2 Phototrophic Sulfide Oxidation

Phototrophic organisms use light energy to fix carbon and can either be photoautotrophic (fix CO_2) or photoheterotrophic (fix organic carbon). Anoxygenic bacteria, such as purple sulfur bacteria, will use reduced sulfur species as electron donors and couple their oxidation with the reduction of CO_2 for energy (equations 1.14-1.18) (Canfield et al, 2005). Oxygenic bacteria, such as cyanobacteria, will couple the oxidation of H_2O to carbon fixation, yielding O_2 as a byproduct. The O_2 produced may be used to oxidize sulfide in the water.

$$CO_2 + 2H_2S \rightarrow CH_2O + H_2O + 2S^0 \quad (1.14)$$
$$3CO_2 + 2S^0 + 5H_2O \rightarrow 3CH_2O + 2SO_4^{2-} + 4H^+ \quad (1.15)$$
$$2CO_2 + H_2S + 2H_2O \rightarrow 2CH_2O + SO_4^{2-} + 2H^+ \quad (1.16)$$
$$CO_2 + 2S_2O_3^{2-} + H_2O \rightarrow CH_2O + 2S^0 + 2SO_4^{2-} \quad (1.17)$$
$$2CO_2 + S_2O_3^{2-} + 3H_2O \rightarrow 2CH_2O + 2SO_4^{2-} + 2H^+ \quad (1.18)$$

Photosynthesis starts with the light harvesting antenna complex of the cell, which surrounds the reaction center where the core processes of photosynthesis take place (figure 1.6). The antenna complex is made up of chlorophyll (Chl), bacteriochlorophyll (Bchl), carontenoids, and phycobilins (Canfield et al., 2005). Light energy is transfered

to the reaction center through chlorophyll or bacteriochlorophyll molecules and stored as excitons (Canfield et al., 2005). In the case of anoxygenic organisms, such as purple bacteria, the excitons excite special pairs of bacteriochlorophyll *a* (P870) molecules in the reaction center changing their electrical potential (E_0') from 0.5 volts to -1.0 volts (figure 1.7A) (Madigan et al., 2002). The excited bacteriochlorophyll *a* molecules become strong electron donors, which drive electron transport and the proton motive forces through cyclic electron flow, subsequently synthesizing ATP (figure 1.6 & 1.7) (Canfield et al., 2005). The bacteriochlorophyll *a* molecules become oxidized to bacteriopheophytin *a* (Bph), which oxidizes further to form quinones (Q) (Canfield et al, 2005). The quinones are collected in a "quinone pool" and used to supply electrons for various reactions, including the reduction of NAD^+ to NADH by reversed electron flow. Cytochromes (transport proteins) are responsible for transporting electrons back to the reaction center, completing the cycle. Cytochrome bc_1 and cytochrome *c* are important for utilizing energy from external electron donors, such as reduced sulfur compounds.

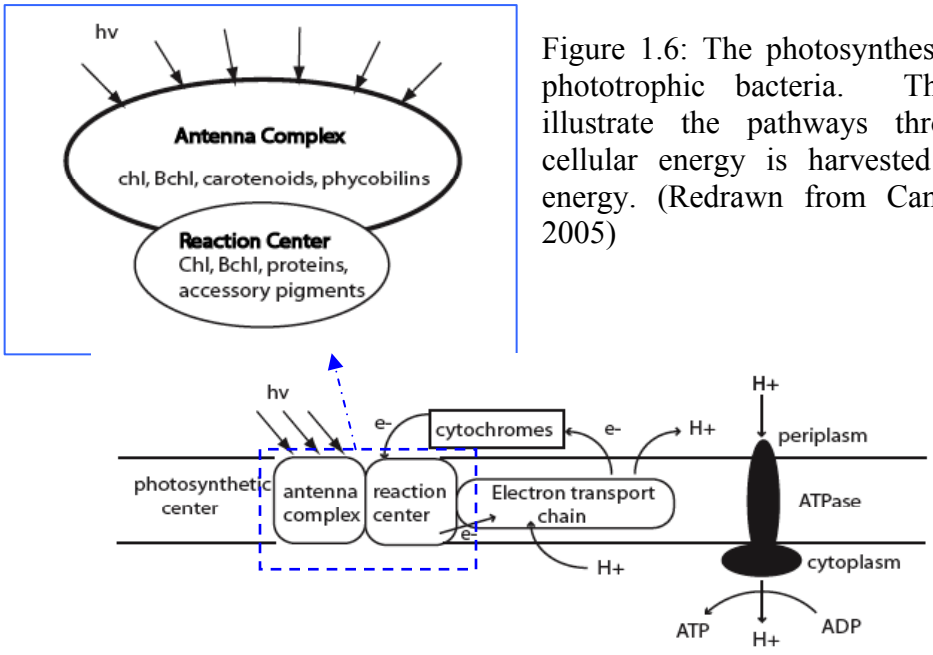

Figure 1.6: The photosynthesis system of phototrophic bacteria. The diagrams illustrate the pathways through which cellular energy is harvested using light energy. (Redrawn from Canfield et al., 2005)

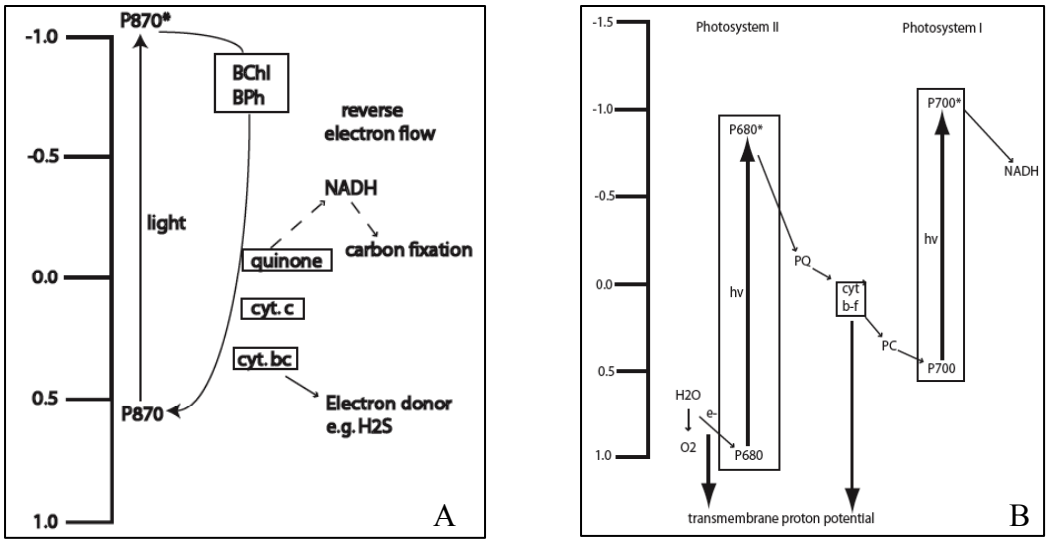

Figure 1.7: With electrical potential on the scale in both A and B, these diagrams illustrate the change in energy assiated with photosynthesis of anoxygenic (A) and oxygenic (B) photosynthesis by cyanobacteria. (Redrawn from Madigan et al., 2005)

In the case of oxygenic phototrophic organisms, like cyanobacteria, chlorophyll is used in two photosystems (figure 1.7B). Photosystem I is characterized by the change in potential of chlorophyll P700 to P700*, and the electrons associated with the reaction are used to convert NAD^+ to NADH. Photosystem II involves the excitement of chlorophyll P680 to P680* (figure 1.7B). The electron lost in this reaction is used reduce the P700* in photosystem I. The P680* of photosystem I is reduced by electrons obtained from the oxidation of H_2O to O_2. H_2S can also be oxidized to SO_4^{2-} by some species of cyanobacteria.

1.5.3 Rates of Sulfide Oxidation

Sulfuric acid speleogenesis is driven by the acid produced through the oxidation of sulfide. The results of a sulfide oxidation model run with Chemical Kinetics Simulator shows the significance of sulfide oxidation to the production of acid (H^+) (figure 1.8). As

HS^- is oxidized by O_2, H^+ and SO_4^{2-} are quickly produced, decreasing the pH. The rate at which sulfide is oxidized is, therefore, related to the rate of speleogenesis through sulfuric acid.

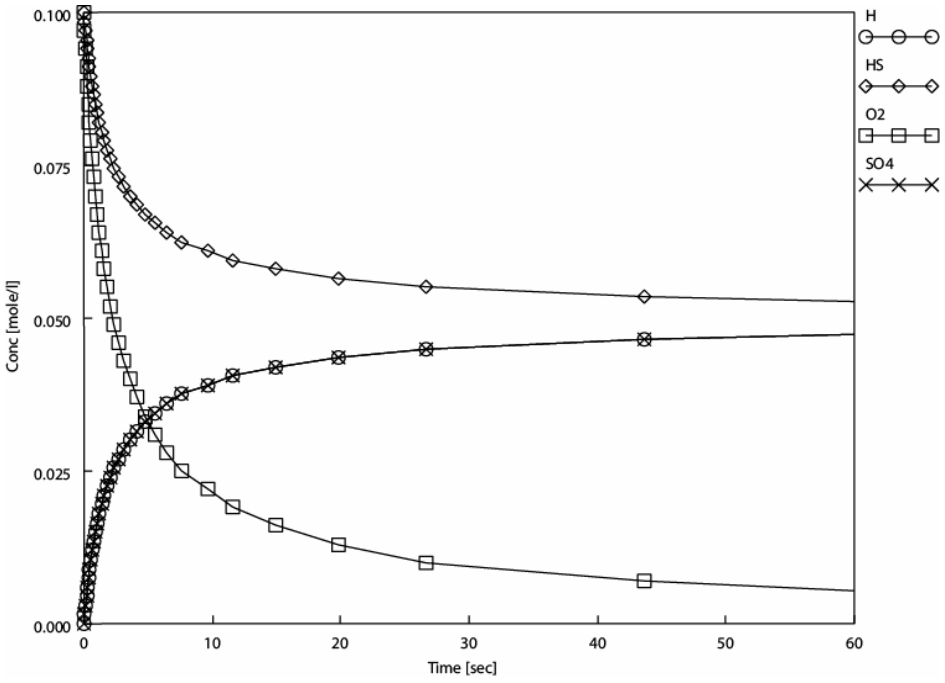

Figure 1.8: Chemical Kinetics Simulator output for a simple model showing the increase in H^+ and SO_4^{2-} as the oxidation reaction of HS^- ($HS^- + 2O_2 \rightarrow H^+ + SO_4^{2-}$) proceeds. This model shows a significant increase in the H^+ concentration as the reaction goes forward.

The rates of sulfur oxidation reactions *in situ* depend on oxygen and reduced sulfur concentration, pH, temperature, ionic strength, and catalysts (such as metals or microorganisms) (Zhang and Millero, 1994; O'Brien and Birkner, 1977; Chen and Morris, 1972; Canfield, 2005). The general equation describing the rate of inorganic sulfide oxidation is given as follows (Canfield et al, 2005):

$$d[H_2S]/dt = -k[O_2][H_2S]_t \qquad (1.19)$$

Intermediate reactions, which are steps in the process of sulfide oxidation (equations 1.5-1.9), complicates the rate at which sulfide is oxidized completely to sulfate. The individual oxidation rates of each intermediate sulfur species formed will affect the overall rate of sulfide oxidation. The following rate equations represent the rate of oxidation of reduced sulfur species, specifically elemental sulfur, polysulfide and thiosulfate (Zhang and Millero, 1994).

$$d[H_2S]/dt = -k_1[H_2S][O_2] - k_3[H_2S][SO_3^{2-}][O_2] \quad (1.20)$$
$$d[SO_3^{2-}]/dt = k_1[H_2S][O_2] - k_3[SO_3^{2-}]^2[O_2]^{0.5} - k_3[H_2S][SO_3^{2-}][O_2] \quad (1.21)$$
$$d[S_2O_2^{2-}]/dt = k_3[H_2S][SO_3^{2-}][O_2] \quad (1.22)$$
$$d[SO_4^{2-}]/dt = k_2[SO_3^{2-}]^2[O_2]^{0.5} \quad (1.23)$$
$$d[S_5]/dt = k_{S5}[S_5]^2[O_2]^{0.5} \quad (1.24)$$

The variability in oxidation rate is represented by changes in the overall rate constant (k), which is derived as a function of pH, temperature, and ionic strength (Zhang and Millero, 1994; O'Brien and Birkner; Chen and Morris, 1972). The following equation was applied to the data obtained from the Frasassi caves to derive the representative rate constant (Canfield et al., 2005):

$$\text{Log}(k) = 11.78 - 3.0 \times 10^3/T + 0.44I^{1/2} \quad (1.25)$$

Sulfur oxidation reactions catalyzed by sulfur utilizing bacteria can proceed through many pathways and can proceed at a rate much faster than inorganic oxidation. The rate of biotic sulfide oxidation is dependent on a number of conditions and is difficult to quantify. The type of sulfur bacteria, the pathways by which sulfide is oxidizes, the cell density within a biofilm, and the oxygen and sulfide concentrations will effect the rate of biotic oxidation (Canfield et al., 2005). The following equation describes biotic sulfide oxidation rates (Canfield et al., 2005):

$$\frac{d[H_2S]_t}{dt} = \frac{-V'_{max}[H_2S][O_2]}{(K_{m\text{-}H2S}[H_2S] + K_{m\text{-}O2}[O_2] + [H_2S][O_2])} \quad (1.26)$$

V'_{max} is the maximum amount of sulfide oxidized (mol 1^{-1} h^{-1}) and can be calculated using V_{max}, the protein content and cell density of the microbial mat (equation 1.27) (Canfield et al., 2005):

$$V'_{max} = V_{max} \text{ x (protein content) x (Cell Density)} \quad (1.27)$$

$K_{m\text{-}H2S}$ and $K_{m\text{-}O2}$ are half saturation constants for H_2S and O_2. $[H_2S]$ and $[O_2]$ denote molar concentrations of total H_2S and O_2 (Canfield et al., 2005).

The rate of oxidation will determine the rate at which sulfuric acid is generated and will influence the rate of cave formation. The oxidation rates should not be used to specifically quantify the rate of speleogenesis; however, oxidation rates are important for understanding the processes and pathways through which sulfuric acid is produced.

Calculations for the rate of H_2S degassing can describe the rate at which H_2S is driven out of the system through oxidation processes and can infer sulfide oxidation rates. Fickian diffusion (equation 1.28) describes complete diffusion of H_2S out of the system using measurements taken at progressive heights above the water/biofilm (Madigan et al., 2002).

$$J=DA((C_1-C_2)/d) \quad (1.28)$$

J denotes the rate of diffusion in mg/s, C_1 and C_2 are measured concentrations of the gas in mg/m^3, A represents the area being studied, d represents the distance between C_1 and C_2, and D is the diffusion constant (0.00001 m^2/s for a simple gas through 1 atm). Canfield et al (2005) presented data showing that, when oxygen and sulfide are at equal

concentrations, the rate of biotic oxidation will be faster than abiotic oxidation when the V'_{max} values are above $1.5 \times 10^{-8} M\ h^{-1}$.

It is important know the distribution of sulfide in order to understand the pathways through which sulfide is oxidized and the redox condition of the environment being studied. This distribution can be expressed in the following mass balance equation (equation 1.29):

$$\Sigma H_2S = mH_2S(initial) - mH_2S(degas) - mH_2S(oxidized) + mH_2S(produced) \quad (1.29)$$

The total H_2S measure in the environment is a function of the initial concentration of sulfide entering the system, the amount of H_2S produced by reducing sulfur bacteria, the flux of the H_2S gas that is leaving the system, and the amount of H_2S that is oxidized through abiotic and biotic pathways. The initial concentration can be measured directly from the source of the sulfidic water entering the environment. The H_2S that leaves the system as gas can also be measured. The amount of H_2S produced and the amount oxidized cannot be individually measured. However, if the mass balance equation is rearranged the amount produced versus the amount oxidized relative to the amount produced can be determined (equation 1.30). This relationship reflects the redox conditions of the environment.

$$\Sigma H_2S - mH_2S(initial) + mH_2S(degas) = mH_2S(produced) - mH_2S(oxidized) \quad (1.30)$$

2.0 Methods

2.1 Analytical Instruments

2.1.1 Electrochemical Analysis: Voltammetry

Electrochemical analysis is a powerful tool in efficiently identifying and quantifying dissolved electroactive species (analytes) in aqueous solutions (Lorenson et al., 2006). Researchers use electrochemical methods to study species of iron, arsenic, manganese, oxygen, and sulfur in natural systems as well as in the lab (Lorenson et al., 2006). The microelectrodes have the ability to simultaneously detect low concentrations of analytes in a given substrate, which gives this technique an advantage over others. Electroanalytical techniques have been applied to an array of environments including submarine vents, Yellowstone hot springs, and cave systems (Lorenson et al., 2006). Information derived from real-time *in situ* measurements can provide a detailed chemical assessment of the aqueous system with respect to changes in chemistry over time and space, and at different pH and temperature conditions. By applying voltammetry (a specific electrochemical technique) to the aqueous environments of the Frasassi cave system, chemical gradients and potential redox reactions were inferred. A detailed description of the microbial ecosystems and geochemical niches were derived using both voltammetry and microbial analysis.

The voltammetric system used in this study is based on three solid-state electrodes: a Au/Hg amalgam solid state working electrode, a platinum wire counter electrode, and a Ag/AgCl reference electrode. Each electrode was constructed in the lab and tested with oxygen, manganese, and thiosulfate.

Analytes in a solution are measured by manipulating an electrical potential between the working and counter electrode. The difference in potential between the two reflects the half reaction taking place on surface of the working electrode. The applied electrical potentials drive redox reactions with the mercury at the 100μM-diameter surface of the Au/Hg amalgam working electrode. The counter electrode serves as a standard and the electrical potential between the working and counter electrodes is recorded. The reference electrode provides a reference against which the difference in the potential between the working and counter electrode can be measured. The electrodes are operated by a DLK60 electrochemical analyzer and its associated software made by Analytical Instrument Systems, Inc. Each species identified is recorded at specific potentials with a specific current (amps) proportional to the concentration of that species in solution.

There are several techniques for manipulating the electrical potential. In this research, cyclic voltammetery was most frequently used. Cyclic voltammetery applies a forward and reverse current from -0.1 V to -1.8 V then back to -0.1 V. The forward current reveals the species in solution and the reverse current can be useful in identifying whether or not a reaction is reversible. The range in potential allows for the simultaneous identification of species in each scan. Square wave voltammetry was occasionally used *in situ* to give supporting evidence for the species identified by the cyclic method. Square wave voltammetry applies the potential in steps and is effective at detecting low concentrations of species.

The entire electrochemical system is easily portable and can be used in many environments given durable accessories. A ruggedized laptop computer and waterproof

case were used for field work in the caves. Working electrodes were transported to and from the field sites in self-designed storage tubes. The tubes were made using 15mL falcon tubes and transfer pipettes. A hole was cut into the top of the 15mL falcon tube into which the transfer pipette was inserted. The top of the pipette was cut off to allow for the holding of the glass working electrode. Liquid electrical tape was used to secure the pipette into the top of the falcon tube. Electrical tape was wrapped around the end of the pipette which was submerged in the falcon tube to ensure little movement of the electrode within the tube. Distilled water was used in the falcon tubes to store the electrodes. This simple case was very effective in protecting the fragile glass electrodes in their travels across the ocean and into the depths of the earth.

2.1.2 Colorimetery and pH measurements

A pH meter was used at each field site to measure the pH and temperature. Before use the pH meter was calibrated with pH 4, 7, and 10 buffers. Temperature and pH measurements were taken in various locations at the sites to detect spatial changes. Field colorimetery was conducted with a Hach portable data logging spectrophotometer to quantify the amount of dissolved oxygen, sulfide, ammonium, and nitrate in the cave water.

2.1.3 Raman Spectroscopy

Raman Spectroscopy was used at Dartmouth College to analyze white biofilm samples collected at Cave Spring. Samples preparations included placing a small amount of biofilm on a thin glass slide and drying. The objective for using Raman measurements

was to determine if elemental sulfur, as well as other species of sulfur, was present in the biofilm samples.

2.2 Field Methods

2.2.1 Vertical and Horizontal Spatial analysis of biofilm mats

Detailed profiles of the biofilm mats and water columns were measured using the glass electrodes, the corresponding voltammetric system, and a micromanipulator. The micromanipulator allowed us to move the glass electrode vertically and horizontally on a sub-millimeter scale yielding detailed profiles. The electrodes were lowered into the water column and into the biofilm mats by intervals of 10μm or greater. At each position into the mat, water column, or sediment, a series of 10 or more voltammetric scans were run to determine the chemistry at that exact location with 100μm diameter precision. Several profiles were taken at each site to determine how the chemistry changes vertically and horizontally within the mat.

2.2.2 Temporal Analysis

In addition to spatial analysis, temporal analysis was also conducted using the glass electrodes and micromanipulator. In active biofilm mats, the working lectrode was positioned in the mat while scans were continuously run for a given amount of time. This showed the changes in chemistry at that particular location over time, suggesting changes in gradient position, microbial activity, or fluctuation in the mats position. Many caves were visited more than once during the two summer field sessions: one in 2005 and one in 2006.

2.2.3 Light Manipulation Experiments

The photosynthetic property of the green sulfur bacteria mat was investigated in 2006 in a light manipulation experiment. A working electrode was set in a steady position inside the mat with the micromanipulator as the amount of sunlight was controlled (figure 2.1). The sulfur chemistry was measured as a function of the amount of light available for photosynthesis. A jacket was held over the mat to provide shade and then removed as constant scans were run for 200 seconds. The response time of the mat to changes in light was tested by spontaneously applying shade to the mat with a hat shortly after the jacket was removed.

Figure 2.1: Pictures showing the set up of the light manipulation experiment at Fissure Spring. (Left) Location of cyanobacteria; (Right) Rain Jacket covering the cyanobacteria

2.3 Lab experiments

2.3.1 Standards

Thiosulfate standards were prepared by mixing Fisher brand $Na_2S_2O_3$ salt in distilled water. Polysulfide standards were made by Lydia Smith following the method presented by Rosen and Tegman (1971) ensuring anoxic storage. The polysulfide standard solution was made by adding hexane-washed salt to N_2-purged distilled water.

The hexane wash ensured that the polysulfide salt was not contaminated with elemental sulfur.

A sulfide standard was made with HS^- salt made by Fisher, Inc. The salt was washed with purged distilled water to remove any oxidized sulfide on the surface. The salt was dried and added to N_2-purged distilled water.

Filters used in the field and in the lab were membrane filters made by Isopore™. The 0.45-µm filter was of type HVLP and the other filters (sizes 0.1-µm, 0.2-µm, and 0.4µm) were of type GTTP.

2.3.2 Testing of electrodes

Before using the electrodes in the field, each was tested in a 1M KCl solution for an oxygen signal. The reaction of dissolved oxygen to peroxide (H_2O_2) first occurs at a potential of -1.4V (figure 2.2). The peroxide is then reduced to H_2O, at a potential of -0.4V (figure 2.2). After testing for an oxygen and peroxide signal the solution was purged and tested with thiosulfate and magnesium standards to eliminate reactions with oxygen as standards were added. The oxygen signals would have also affected the current (peak height) and potential of the standard measurements if the solution was not purged. Thiosulfate and magnesium were added to the solution in micro-molar increments. Thiosulfate and manganese was useful in determining the quality of the electrode because their signals are at each end of the potential range; thiosulfate has a potential of -0.2V and manganese has a potential of -1.7V.

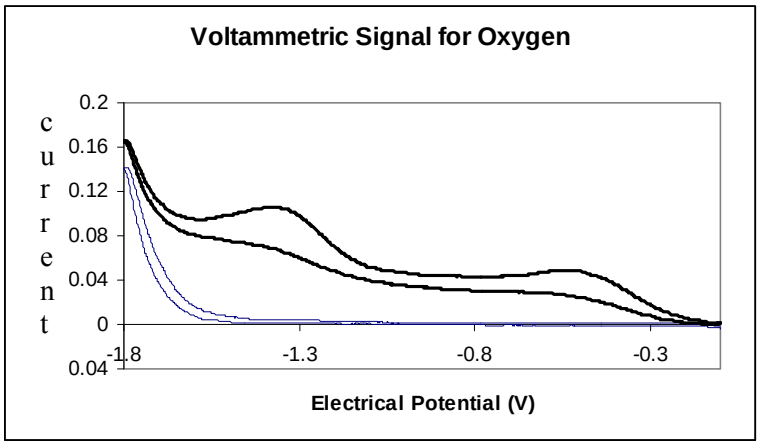

Figure 2.2: Voltammetric scan of the standard Cave Spring water showing good oxygen (-1.4 V) and peroxide (-0.4 V) signals. The Cave Spring water was then purged with nitrogen gas to get rid of the dissolved oxygen. The result of the purged water shows to be flat, indicating a good working electrode. Current is measured in µAmps.

2.3.3 Identification of sulfur species

In order to identify and quantify chemical species *in situ,* standards were analyzed with the microelectrodes under conditions similar to those *in situ*. The potential for the sulfur species observed *in situ* were known based on previous work (Lorenson et al., 2006). However, each natural system has a unique pH, temperature, organic, and inorganic chemistry that may alter the signal of each species. For example, sulfide will shift to a more negative potential as a function of decreasing pH. Also, the solubility of different species, such as elemental sulfur, may be influenced by the organic chemistry. Thiosulfate, polysulfide, elemental sulfur, and sulfide standards were identified in a water sample collected from the field site referred to as *Cave Spring*. The Cave Spring water had a neutral pH and was stored at room temperature. This water was used to represent the sulfidic water running through the Frasassi cave system.

Sulfide was calibrated in the Cave Spring water by adding sulfide to the Cave Spring water at 50uM intervals. The results of this calibration were plotted in Excel®, from which a linear calibration was determined. This linear calibration was used to quantify the *in situ* sulfide measurements.

2.3.4 Elemental sulfur solubility experiments

Lab experiments were conducted to investigate the solubility of elemental sulfur and to identify the voltammetric signals for the two forms of elemental sulfur observed in aqueous environments (colloidal and dissolved) (Steudel and Holdt, 1988; Wang et al., 1998). The goal of these experiments was to dissolve the elemental sulfur in solution, differentiate between the two signals, and define the size of the colloidal and dissolved species. The results of the experiments were applied to interpret *in situ* measurements of sulfur.

Initial experiments were based on sulfur solubility experiments conducted by Steudel and Holdt (1988) using various organic surfactants. These experiments focused on dissolving sulfur in organic-rich water. Sodium dodecyl sulfate (SDS) [$C_{12}H_{25}SO_4Na$], n-hexadeyltrimethylammonium bromide (CTAB) [$CH_3(CH_2)_{15}N(CH_3)Br$], and methanol [CH_4] were used to investigate the solubility of precipitated sulfur (S). Solutions were made with one gram of each organic surfactant in distilled water. One gram of precipitated sulfur was added to a solution of the organic surfactant solution. The solutions were stirred for variable amounts of time (minutes, hours, and days) in an effort to dissolve the maximum amount of sulfur. The sulfur

chemistry of the solutions made was analyzed with voltammetry using solid state Au/Hg electrodes.

To further investigate the voltammetric signals of elemental sulfur and its solubility in water, polysulfide was acidified in the presence of the organic surfactant (SDS). The acidification of polysulfide yields the formation of colloidal sulfur particles (Wang et al., 1998). The formation of elemental sulfur upon acidification was obvious by the change in the color of the solution from clear to cloudy white. This method of dissolving sulfur may be more effective than previous experiments based on the property that the sulfur produced during acidification would already be suspended in solution and may be much smaller than the precipitated sulfur used before. Wang et al. (1998) found the acidification method to be successful at solublizing elemental sulfur in the presence of ethanol.

The dissolution experiments conduced by Lorenson et al. (2006) presented evidence that the voltammetric signals for colloidal and dissolved sulfur were size dependent through filtering the sulfur/SDS solution. Later attempts were made to repeat Lorenson's experiments by applying different sized filters to the variety of sulfur solutions created. Solutions of SDS with the elemental sulfur derived from the various techniques (i.e. acidification) were filtered using four filters of differing sizes: 0.45μm, 0.4μm, 0.2μm, and 0.1μm filters. The solutions were measured before and after filtration to attempt to identify the two species of sulfur and to determine their size dependence. It is important to note that the structure of the 0.45μm and 0.4μm filters were different and might have had an effect on filtration as a function of size.

3.0 Results

3.1 Lab Experiments

3.1.1 Elemental Sulfur: Colloidal vs. Dissolved

Lab experiments were conducted in an effort to better understand the two forms of sulfur detected *in situ*. The goal of these experiments was to decipher between dissolve and colloidal sulfur in solution. The dissolution of elemental sulfur was attained using several techniques after Lorenson et al, 2006, Steudel et al 1988, and Wang et al., 1998. The results showed that SDS dissolves elemental sulfur the most efficiently. It was observed that before SDS was applied to elemental sulfur solutions no signal is detected at -1.2 V, only a signal at -0.8 V. When SDS was present in the solution the signal at -1.2 V occurs. This pattern was observed for all three techniques for dissolving elemental sulfur with SDS: with precipitated sulfur, acidified polysulfide and acidified thiosulfate.

The size of the colloidal sulfur particle detected in solution was investigated through filtering the solutions with different sized filters: 0.45-µm, 0.40-µm, 0.2-µm, and 0.1-µm. The results showed that the size and type of filter was not significant in determining the size range. Lorenson et al. (2006) showed that the peak at -0.8 V would disappear upon filtration with a 0.45-µm filter. However, in these experiments the -0.8 V peak never disappeared as a result of filtration. Instead, the peak at -1.2 V repeatedly vanished as a function of filtration in many but not all cases. The disappearance of the -1.2 V peak upon filtration was consistent with most solutions made through the various techniques of dissolving elemental sulfur. It was, however, observed that the existence of the peak at -1.2 V was dependent on the presence of an organic compound. The

following graphs show the results of the elemental sulfur solubility and filtration experiments (figures 3.1-3.4).

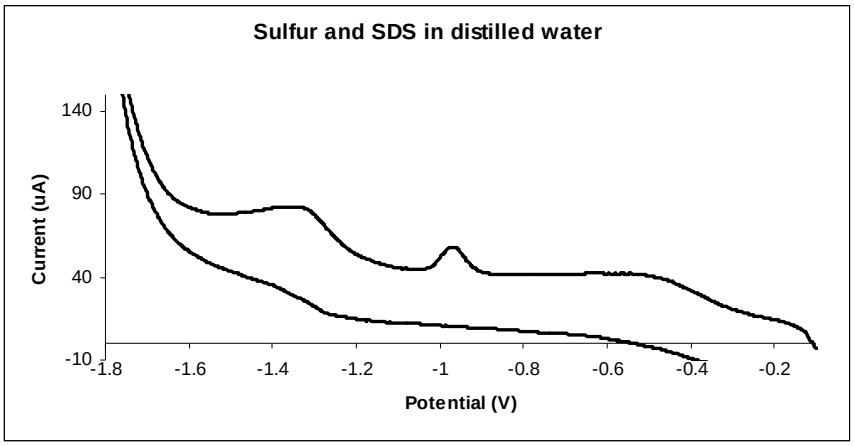

Figure 3.1: Voltammetric scans (CV 1 V/s) of a SDS and precipitated sulfur solution made in distilled water. The peaks represent colloidal and dissolved sulfur of unknown concentrations. The peaks appear at more negative potentials because the solution was made in distilled water and had a low concentration of ions.

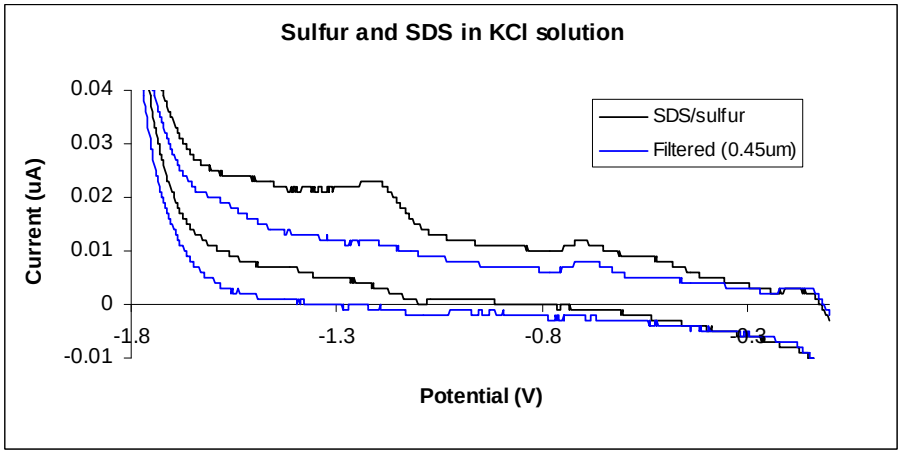

Figure 3.2: Voltammetric scans (CV 1V/s) of a SDS and precipitated sulfur solution made in 0.1 M KCl. The peaks at -1.2 V and -0.7 V represent the colloidal and dissolved sulfur in solution. The solution was filtered with a 0.45-µm filter resulting in the disappearance of the peak at -1.2 V.

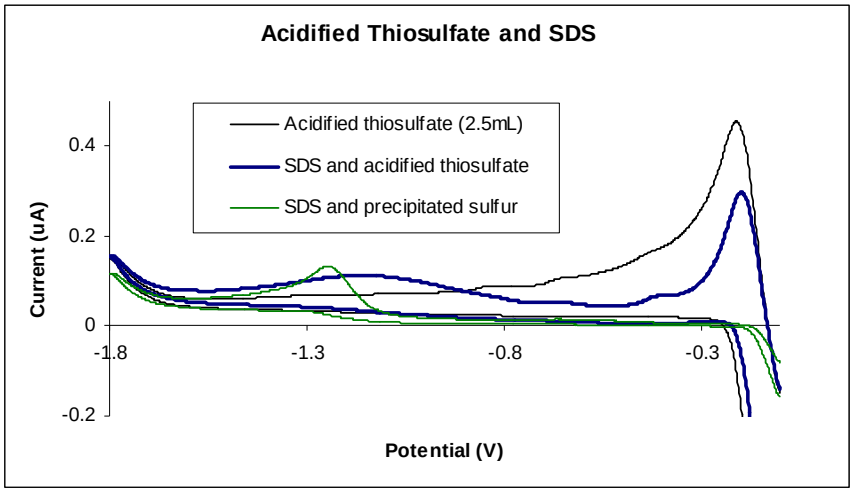

Figure 3.3: Voltammetric scans (CV 1V/s) of acidified thiosulfate solution. SDS was added to the acidified thiosulfate resulting in a peak at approximately -1.2 V. The peak at -1.2 V is consistent with the -1.2 peak observed with the SDS and precipitated sulfur solution.

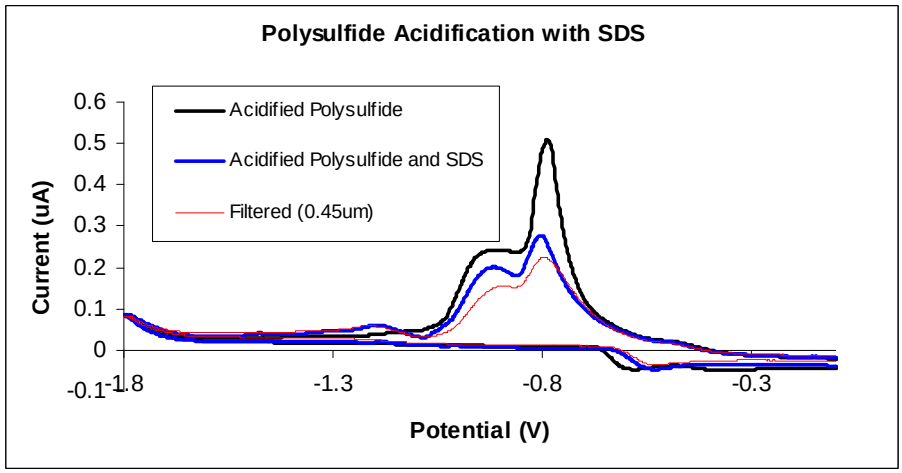

Figure 3.4: Voltammetric scans (CV 1V/s) of the acidified polysulfide solution. SDS was added to the solution resulting in a peak at -1.2 V. When filtered with a 0.45-µm filter, the -1.2 V peak did not disappear, unlike with filtering other solutions (figure 3.2).

3.1.2 Sulfide Calibration

Sulfide was calibrated in the Cave Spring water and then applied to the *in situ* measurements in order to quantify changes in sulfide concentrations. A linear calibration between peak height and concentration was found using Excel®. It was determined that a sulfide calibration for specific ranges in concentrations required three linear calibrations. As the concentration of HS^- increases, HS^- is loaded onto the electrode surface, changing the slope of the linear calibration. Table 2 shows these linear calibration lines determined for the relationship between sulfide and peak height or current. The linear calibrations were applied to many of the *in situ* voltammetric measurements to quantify the sulfide concentration. Other voltammetric measurements were interpreted by simply comparing changes in the current, knowing that current represent concentration.

Concentration Range	**nAmp Range**	**Equations**
<10uM	<40	y = 0.2326x
<100uM	40-217	y = 0.5102x - 20.763
100uM-200uM	217-394	y = 0.5649x – 22.3
>200uM	394>	y = 1.5586x - 426.74

Table 2: These linear calibrations of Au/Hg electrodes in Cave Spring water show concentration (μM) vs. current (nAmps) for the HS^-. These equations were applied to quantify sulfide *in situ.*

3.1.3 Polysulfide vs. Sulfide

The polysulfide and sulfide signals in simple solutions, free of other sulfur species, are distinctly identified: polysulfide at -0.8 V and sulfide at -0.9 V. However, the signals of polysulfide and sulfide are not well understood when they coexist solution. The signals for polysulfide and sulfide have close but separate potentials when measured

individually in Cave Spring water (figure 3.5). When sulfide and polysulfide are together in solution only one peak is observed. The distinction between polysulfide and sulfide is further complicated in the presence of elemental sulfur and other sulfur species. In many sulfidic environments the electrodes show a "triple peak" which we have assumed to represent three species: sulfide, polysulfide, and elemental sulfur (figure 3.6). For the research on the cave system we will assume the peak observed at -0.9 V is sulfide, and sulfur species of the triple peak are that of sulfur, polysulfide, and sulfide. It is important to keep this assumption in mind when interpreting the data.

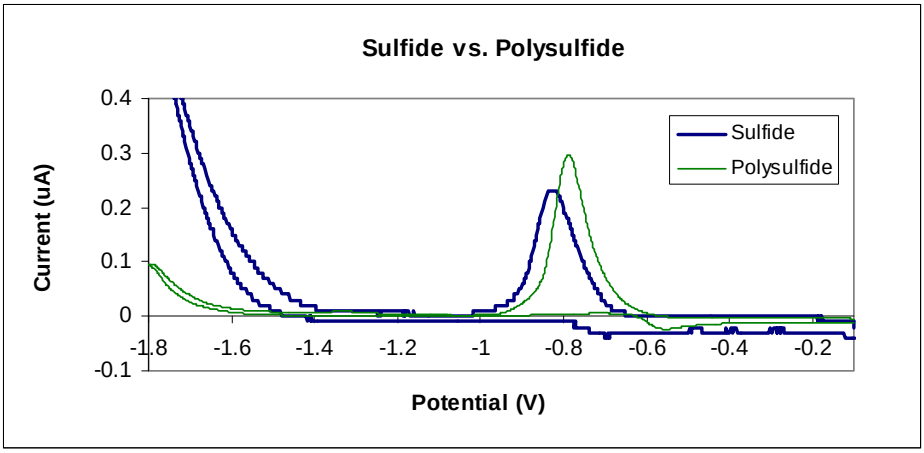

Figure 3.5: Voltammetric scans (CV 1V/s) showing the difference between sulfide (100uM) and polysulfide (100uM) potentials. As concentrations increase, these peaks will shift negatively and may switch order. For instance, in the triple peak polysulfide is more negative than sulfide (figure 3.6).

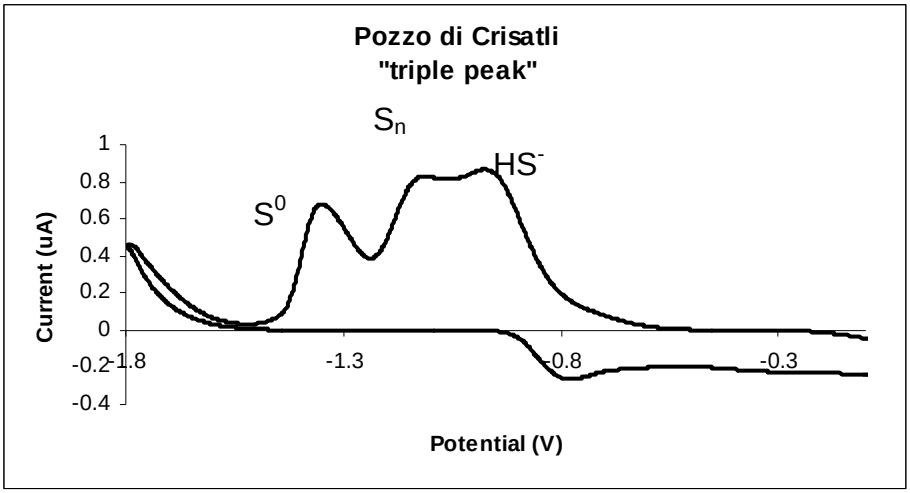

Figure 3.6: Voltammetric scan (CV 1V/s) showing the "triple peak" of elemental sulfur (S^0), polysulfide (S_n), and sulfide (HS^-). This scan is a measurement taken from Pozzo di Cristali in 2005, 7mm into the thick white biofilm mat in the stream. The polysulfide (S_n) peak around -1.0V is a subject of uncertainty and further investigation.

3.2 Field Data

3.2.1 Cave Spring

Sulfidic waters exit the Frasassi cave system in to the Sentino River at the site referred to as Cave Spring. Cave Spring is a small cave occupied by stream and white fluffy biofilm mats (figure 3.7). The in the stream was a mixture of meteoric water and deep sulfidic groundwater which runs through the caves. The water had a neutral pH and a temperature of about 14º C. The biofilm mats at this site were mostly comprised of δ-proteobacteria (Figure 3.7), which was determined through genomic analysis by Dr. Jenn Macalady at Penn State University. It was difficult to measure a profile of the white mat because of its dynamic behavior in the water. As shown in figure 3.7, the white mat was attached to a rock at one end and moved fluidly with the water. Profiles taken in 2005

and 2006 show that sulfide sharply decreased into the mat and increased as the electrode was lowered through the mat and into the underlying water (figure 3.8 and 3.9).

The Raman Spectroscopy results for a Cave Spring biofilm sample revealed that elemental sulfur was present.

Fig 3.7: (Left) Picture of Cave Spring and voltammetric set up. (Right) Picture of the glass working electrode measuring into the feathery white biofilm as it flowed downstream.

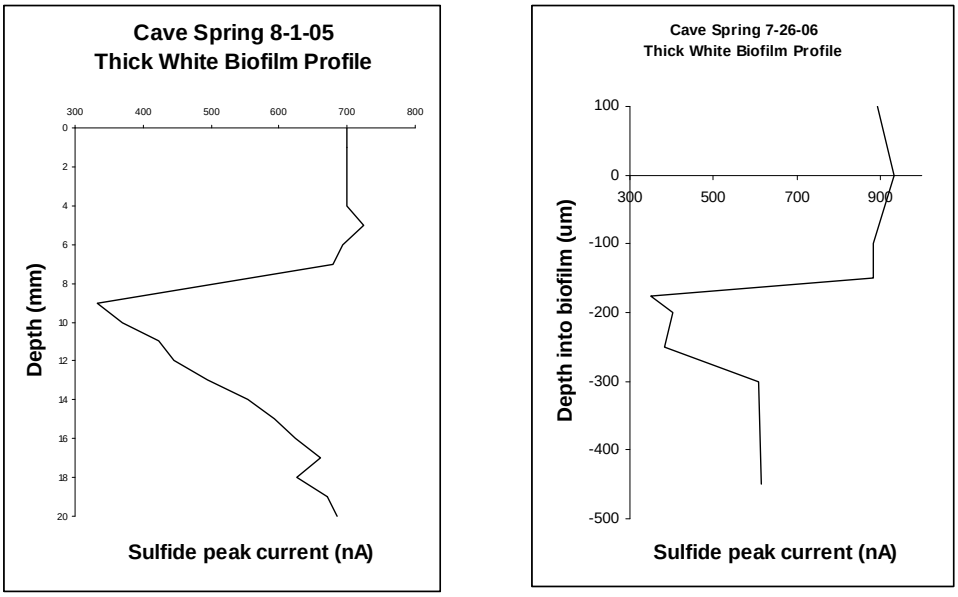

Figure 3.8: Two profiles of sulfide into the white biofilm at the Cave Spring site. Sulfide concentration is presented as current (nA), which is proportional to concentration.

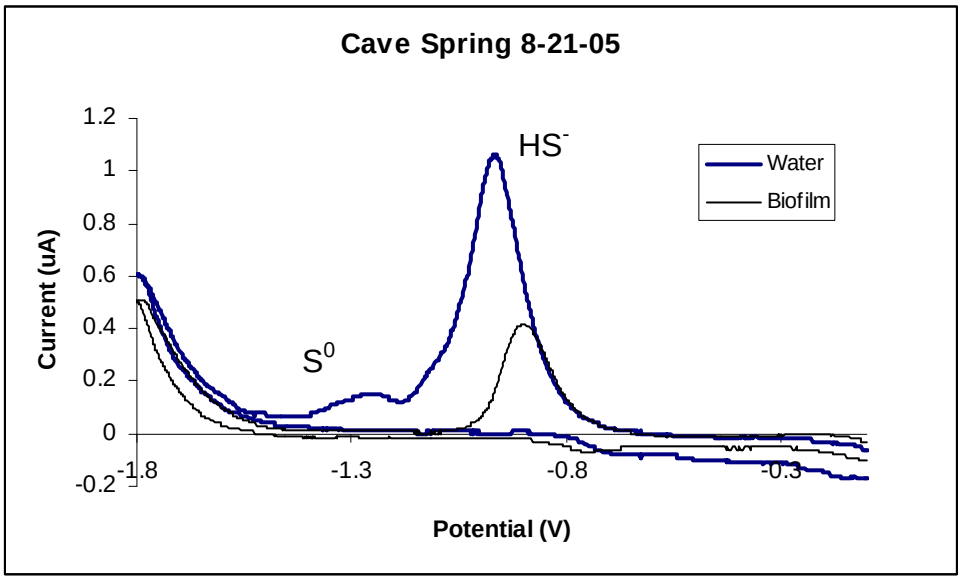

Figure 3.9: Representative voltammetric scans (CV 1V/s) of the change in sulfur chemistry between the bulk water and the biofilm. The water measurement was taken just above the biofilm/water interface. The biofilm measurement was taken 200µm into the biofilm.

3.2.2 Lago Verdi

Lago Verdi is a room in the Grotta del Fiume cave with a small stagnant body of sulfidic water. The water temperature was 13.7ºC and the pH ranged from 7.4 to 7.2. No obvious microbial communities were present in this aqueous environment. The electrodes were used to measure the chemistry of the water and of the fine grained black sediment at the bottom of the water column. This fine black mud was not observed at other sights we visited within the cave.

The voltammetric measurements show that elemental sulfur, sulfide, and polysulfide were all present in the water column and in the sediment. It was observed with CV 1V/s voltammetric scans that the HS^- oxidizes forming polysulfide and

elemental sulfur in the surface water (figure 3.10). The sediment/water interface showed an increase in polysulfide and elemental sulfur from the mostly sulfidic water. The polysulfide and elemental sulfur, however, decreased slightly with depth into the sediment.

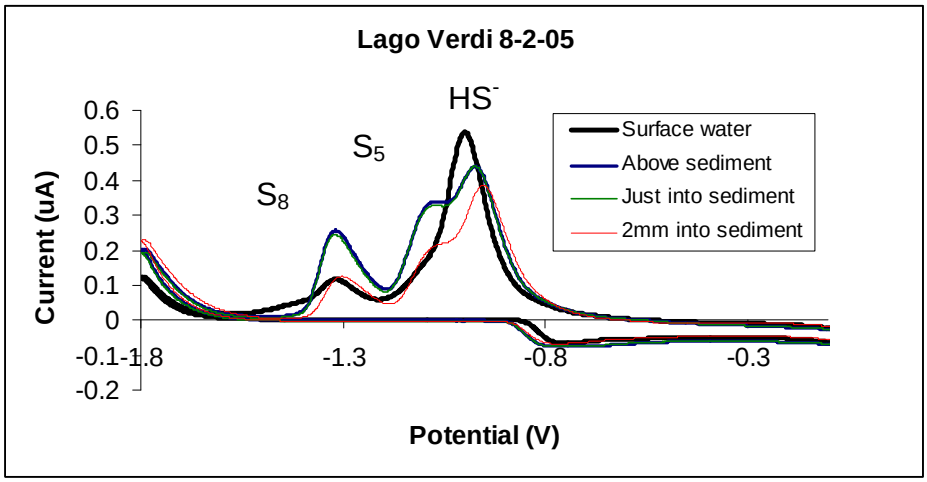

Figure 3.10: Voltammetric scans (CV 1V/s) showing a profile of the water column and sediment at Lago Verdi. Sulfide and elemental sulfur are present in the surface water and oxidize further down. Polysulfide and elemental sulfur are products of this oxidation and decrease in concentration with depth into the sediment.

3.2.3 Grotto Sulfureo

Grotto Sulfureo is located in a different arm of the cave system from the other sites visited. Thin white mats dominated by *Beggiatoa spp* occupied the top of a small body of water. A profile was taken of the *Beggiatoa spp* mats, although it was difficult to stabilize the working electrode in the mats because they were very thin. The chemistry at Grotto Sulfureo did not vary as a function of depth within the water column through the biofilm (figure 3.11). Elemental sulfur and sulfide were the species of sulfur measured.

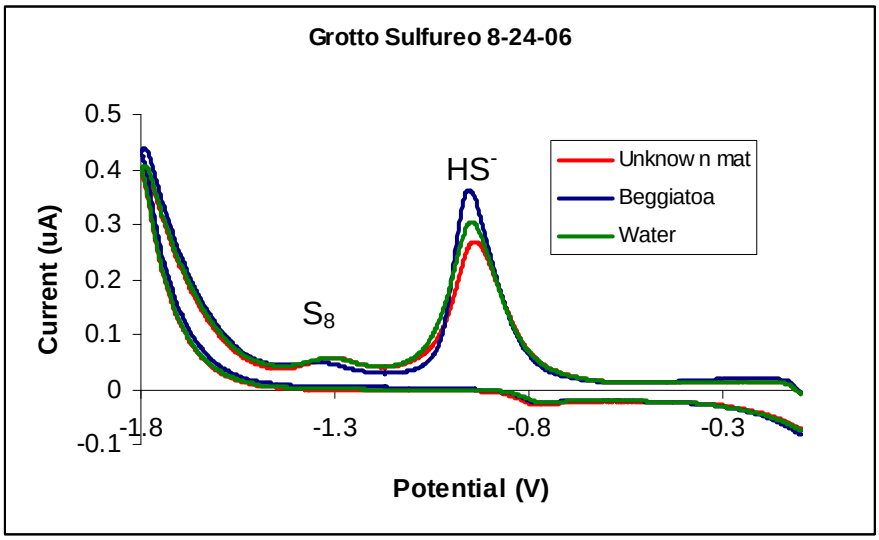

Figure 3.11: Voltammetric scans (CV 1V/s) comparing the two mat types observed at Grotto Sulfureo and the surface water chemistry.

3.2.4 Ramo Sulfureo

Ramo Sufureo, located in the section of Grotta del Fiume, was the deepest section of the cave visited during the two summers of research. A variety of microbial communities inhabited Ramo Sulfureo, including ones dominated by *Beggiatoa spp*, δ-proteobacteria, and Snottites.

The chemistry associated with the *Beggiatoa spp*-dominated biofilm is presented in figure 3.12. The chemistry does not change with depth into the mat and water column; however, the mats were so thin that a significant vertical profile of the mat itself could not be measured. The profile of the water column associated with the *Beggiatoa spp* shows a small change in sulfide, thiosulfate, and elemental sulfur with depth. It also appears that the polysulfide concentrations were low.

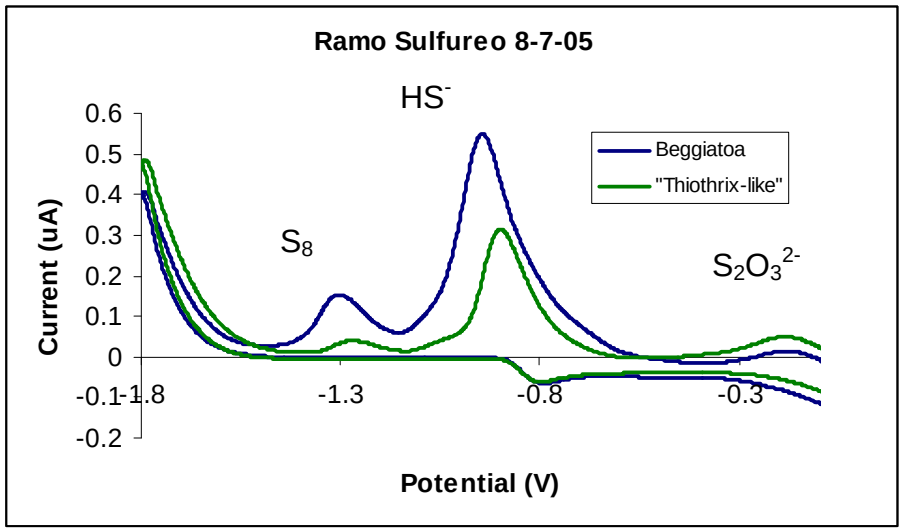

Figure 3.12: Voltammetric scans (CV 1V/s) comparing the two biofilm mats observed at Ramo Sulfureo in 2005. The chemistry is dominated by sulfide, elemental sulfur and thiosulfate.

Ramo Sulfureo also had thin, white, feathery biofilms. These feathery mats are known to be similar to thiothrix and dominated by δ-proteobacteria. The thiothrix-like biofilms were attached to the rock and flowed freely in the water. This behavior is similar to the δ-proteobacteria dominated biofilm in Cave Spring, although the Ramo Sulfereo biofilm was much thinner. The profile of these mats reveals relatively heterogeneous sulfur chemistry, consisting of elemental sulfur, sulfide, and thiosulfate (figure 3.12).

In addition to studying aqueous microbial communities, we were able to analyze snottites found on the Ramo Sulfureo walls. Snottites often exist on gypsum crystals (figure 1.3) and were abundant, but not limited to Ramo Sulfereo. Hundreds of snottites were collected in 1.5mL eppendorf tubes, to which voltammetry was applied. Several sequences of voltammetric scans were taken by simply holding the electrodes in an

eppendorf tube containing a snottite sample. The measurements revealed a high concentration of sulfide.

The pH of the snottites was very low, shifting the sulfide potential from around -0.8 to -0.45V (figure 3.13). The pH could be determined using the voltammetric scans because of the relationship between electrical potential and pH, which was calibrated by Lorenson et al. (2006). This calibration was used to estimate the pH of the snottites, which was around three. This was confirmed with *in situ* applications of pH paper, further supporting the pH predicted by voltammetry.

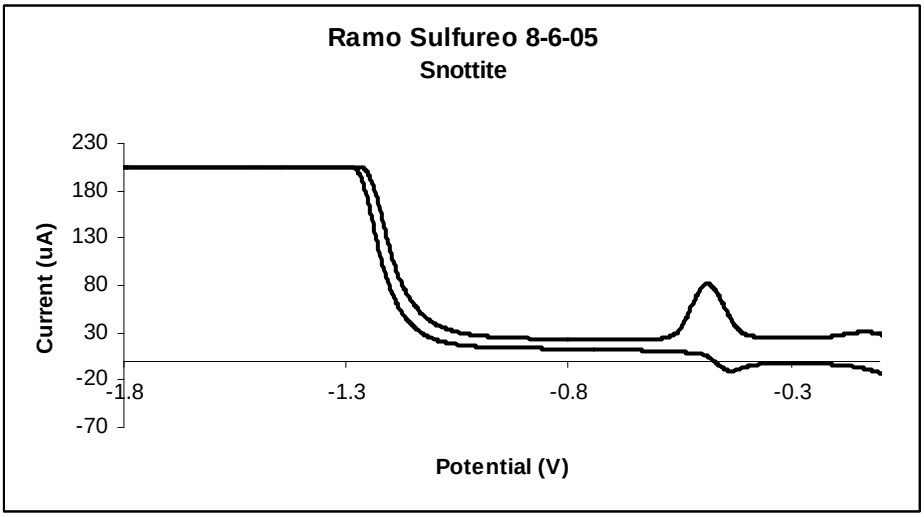

Figure 3.13: Voltammetric scan (CV 1V/s) of snottites collected in a 1.5mL ependorf tube. The potential of the sulfide peak indicates a low pH, which was determined to be three.

3.2.5 Pozzo di Cristali

3.2.5.1 Observations

Pozzo di Cristali is a long, narrow passage about ten minutes walking distance from the main entrance. A slow-flowing, 2.5 by 7 meter stream ran through this passage and was inhabited by a fluffy, thick, white biofilm mat (figure 3.14). This biofilm was dominated by δ-proteobacteria, as determined from previous research (Macalady et al, 2006). Very thin white mats were also studied at the far end of the stream and are different from the fluffy white mats upstream (figure 3.14). The thin white mats were dominated by *Thiovulum spp* and existed in calm water about seven meters downstream from the stream orifice. In 2006 the water height was lower and there appeared to be a decline in the extent of biofilm in the stream compared to 2005.

3.2.5.2 Lateral Spatial Analysis

The rate at which the white biofilm oxidizes sulfide was investigated through the spatial analysis of the water and biofilm as the sulfidic waters passed downstream through the mat. In 2005, three locations were chosen along the mat and measured with the electrodes. The data obtained from this investigation is presented in figures 3.15 and 3.16 and shows that sulfide and elemental sulfur did decrease as a function of flow. Spatial analysis was conducted in 2006 with more detail, as several measurements were taken along the thick white biofilm in the stream (figures 3.14-3.16). It is also important to note that the chemistry from 2005 was more diverse; there was elemental sulfur and polysulfide present in addition to the sulfide. In 2006, only sulfide was detected.

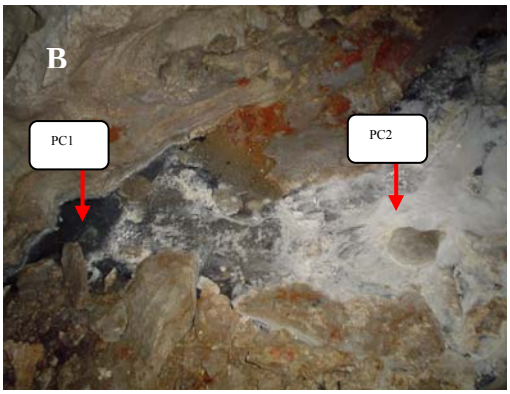

Figure 3.14: The stream running through Pozzo di Cristali, inhabited by a thick white biofilm (A). Several sites were measured downstream, starting with the orifice (PC1) (B). PC2 represents the location of the next measurement, taken in 2005 (B). Picture (C) shows the *Thiovulum* mat at the end of the stream, representing the final measurements of the lateral sequences in 2005 and 2006.

A

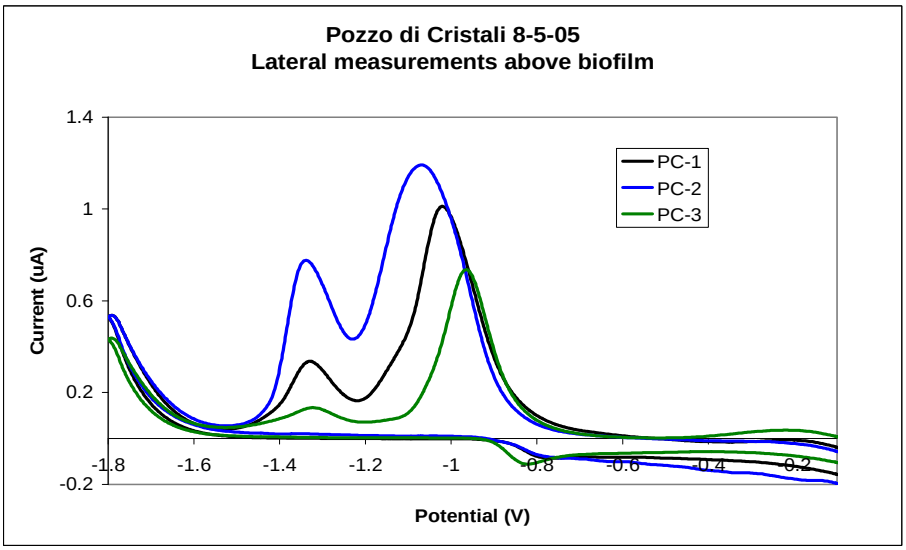

B

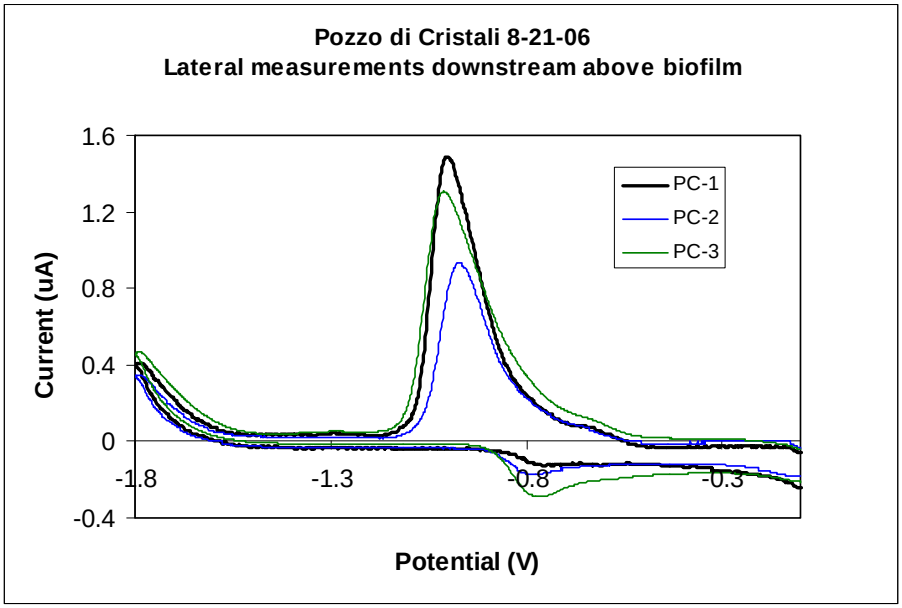

Figure 3.15 Voltammetric scans (CV 1V/s) taken at three locations along the stream at Pozzo di Cristali. The scans were taken just above the biofilm mats the orifice (PC-1), 0.2 meters downstream from the orifice above the thick white mat (PC-2), and 5-7 meters downstream above the *Thiovulum* mat (PC-3).

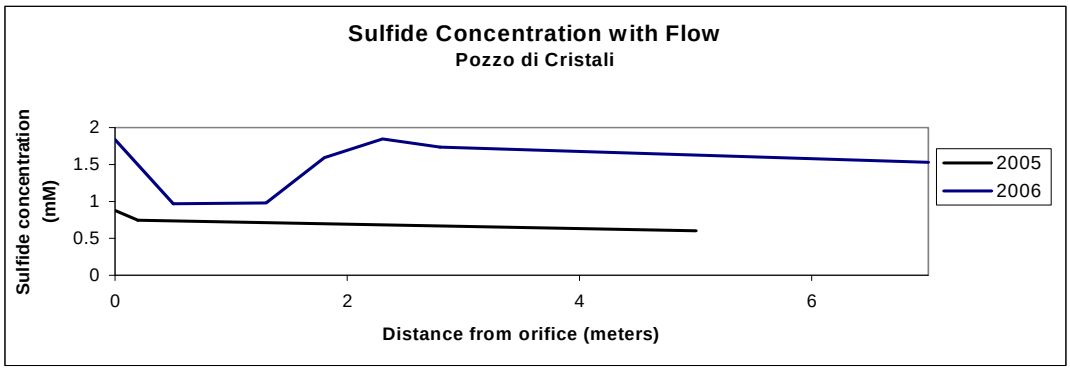

Figure 3.16: The change in sulfide concentration along the stream at Pozzo di Cristale. These measurements were taken in the water and in the biofilm in 2005 and 2006.

3.2.5.3 Vertical profile

Vertical profiles of the white biofilm show the changes in sulfide chemistry with depth. As shown in the lateral data, there is a drastic difference in the chemistry between 2005 and 2006 (figure 3.15 & 3.16). This difference was also presented in the vertical profiles. In 2006 only sulfide was detected, whereas in 2005 sulfide, polysulfide and elemental sulfur were detected (figure 3.17). In the 2005 measurements, sulfide decrease sharply around -7mm depth into the biofilm mat (figure 3.17). This sharp decrease was coupled with an increase in polysulfide and elemental sulfur, which were products of sulfide oxidation.

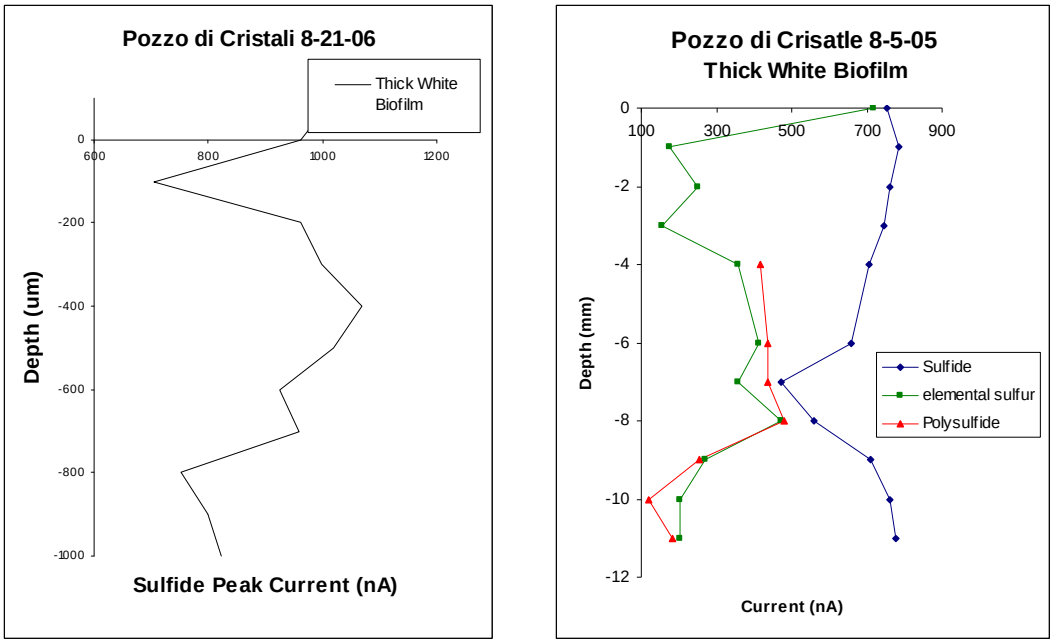

Figure 3.17: Profiles of the thick white biofilm observed at Pozzo di Crisatle. The profiles were taken in 2005 and 2006 and show a difference in the chemistry between the two years.

It was difficult to obtain a detailed profile of the thin white *Thiovulum* because it was so thin. However, the profile of the water column was significant to our understanding of the *Thiovulum* community. As seen in figure 3.18, there was no sharp change in sulfide or elemental sulfur, unlike in the thicker white mat. In 2005 polysulfide and elemental sulfur were detected in association with the *Thiovulum* mat (figure 3.18); however, in 2006 only sulfide was detected.

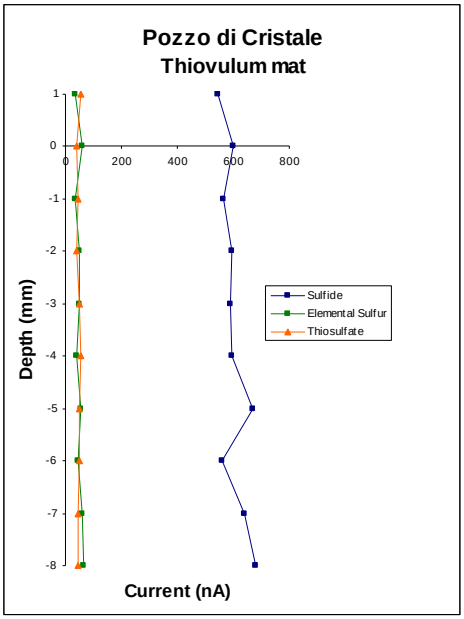

Figure 3.18: Profile of the water column inhabited by a *Thiovulum* mat at Pozzo di Crisatli in 2005.

3.2.5.4 Rates of Oxidation at Pozzo di Cristali

Qualitative analysis of sulfide oxidation was based on interpreting changes in the sulfide and intermediate sulfur species over time and space. General observations about the slope of the redox gradients and the types of species present in the environment were evidence for sulfide oxidation. In order to quantify the rate of sulfide oxidation, abiotic and biotic rates of sulfide oxidation were calculated from the data obtained from Pozzo di Cristali in 2005. These calculations predicted the rates of oxidation for the environment measured and were compared to the rates of oxidation directly measured *in situ.* Sulfide concentrations were derived using the linear calibration curves derived in the lab (table 2). Oxygen measurements taken by Jenn Macalady using field colorimetry were also used in these calculations. Data from 2006 was not included because the biofilm in the stream was not actively oxidizing sulfide. Canfield et al., 2005 provided values for

various constants that could not be measured. Table 3 presents the field data and known data used for in calculations.

$[H_2S]_i$ (M)	881.35	**$[O_2]_I$ (M)**	5.175
$[H_2S]_f$ (M) (above mat)	598.17	**$H_2S]_f$ (M) (-1m in mat)**	103.1078
$C_1(H_2S_{(g)})$ (mg/m^3)	6.2	**C_2 ($H_2S_{(g)}$) (mg/m^3)**	0.2
Log K	1.614	**I**	0.1
d (m)	5	**Flow rate cm/s**	5.92
Area of stream (m^2)	1.	**D (m^2/s)**	.00001
V'max (M/h)	1.5×10^{-3}	**$K_{m\text{-}H2S}$ (M)**	7.4×10^{-5}
$K_{m\text{-}O2}$(M)	1.5×10^{-6}	**T (ºC)**	13.2

Table 3: Summary of field data. The constants V'_{max}, $K_{m\text{-}o2}$, $K_{m\text{-}H2S}$, and D were taken from (Canfield et al., 2005).

Data from table 3 was inputted into equations 1.19, 1.26-1.29, & 2.0 to understand the rate at which sulfide was oxidized. Equation 1.19 predicted the abiotic sulfide oxidation to be 0.13uM/s. In contrast, the biotic prediction (equation 1.26) was 0.03uM/s, which is an order of magnitude slower than the abiotic rate. The rate of hydrogen sulfide gas diffusion out of the aqueous system based on field data was found to be 1.23×10^{-3}uM/s (equation 1.28) and was based on field data. The *in situ* rate of oxidation was calculated from the change in sulfide concentration downstream, flow of the stream, and distance measured (equation 2.0). The results of all calculations are presented in table 4.

$$d[H_2S]/dt = ([H_2S]_f - [H_2S]_i)/(\text{flow x distance}) \qquad (2.0)$$

The rate of *in situ* oxidation was found to be the faster rate, followed by the abiotic prediction and biotic prediction. The rate of hydrogen sulfide diffusion out of the aqueous system was much slower than the other rates.

Rate (Abiotic) (equation ##)	-0.13
Rate (Biotic) (equation ##)	-0.03
J	1.23×10^{-3}
***In Situ* rate above biofilm**	-3.4

Table 4: Summary of rate calculation results. All rates are in μM/s.

3.2.6 Phototrophic Bacteria

3.2.6.1 Cyanobacteria: Fissure Spring

Fissure Spring is another exit of sulfidic water from the caves. At this site, sulfidic water directly enters the Sentino River, creating conditions favorable for photosynthetic sulfur-utilizing biofilm mats. Green phototrophic mats were observed in calm waters adjacent to the spring orifice. These green mats are known to be comprised of cyanobacteria, which was determined in previous studies (Macalady et al., 2005). The cyanobacteria at Fissure Spring seem to use sulfide as an electron donor instead of water. The mat exists on the sediment-water interface. The underlying sediment is a fine black mud and is rich in organic material. Profiles were taken with the electrodes and were able to show that these mats are oxidizing sulfide and elemental sulfur (figure 3.19). The point at which a sharp decline in sulfide concentration occurs is observed to be associated with an increase in thiosulfate. Elemental sulfur was also measured, although only in small concentrations.

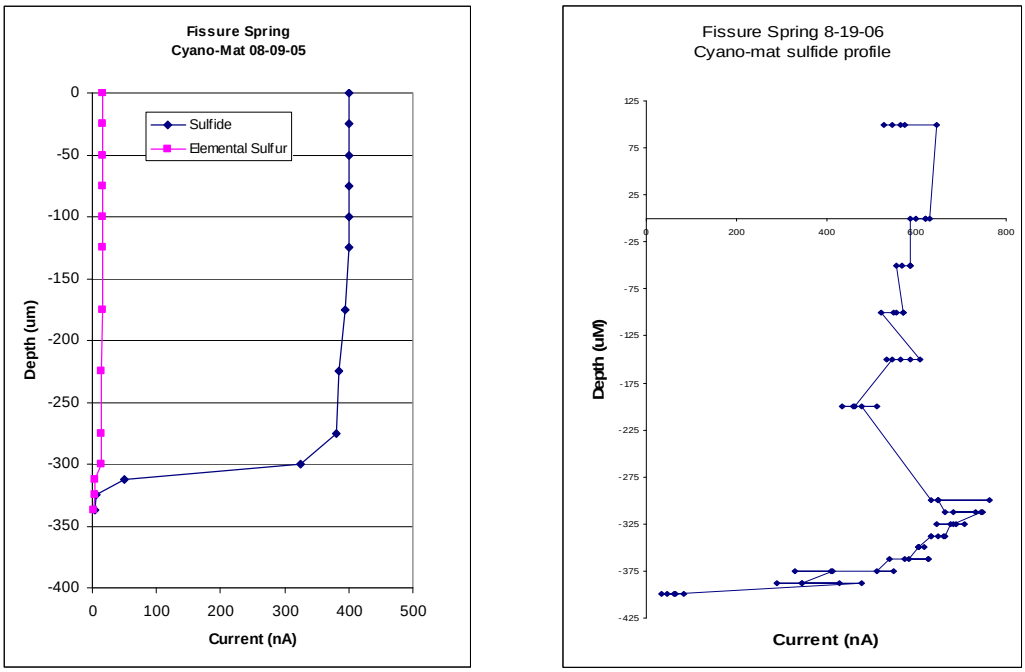

Figure 3.19: Profiles of the cyanobacteria at Fissure Spring showing a steep sulfide gradient. It is important to note that these profiles were taken when the mat was covered with shade.

The photosynthetic property of the green sulfur bacteria mat was investigated in 2006 in a light manipulation experiment. The sulfur chemistry was measured as a function of the amount of light available for photosynthesis. A jacket was held over the mat to provide shade and then released as constant scans were run for 200 seconds (figure 3.20). For the first 80 seconds the jacket was held over the site (figure 3.20). Shade was applied around 130 seconds and 180 seconds. This was observed by an immediate increase in sulfide. There is a pattern of decreasing concentration of sulfide with photosynthesis and an increase without photosynthesis, implying a dependence on photosynthesis for sulfide oxidation.

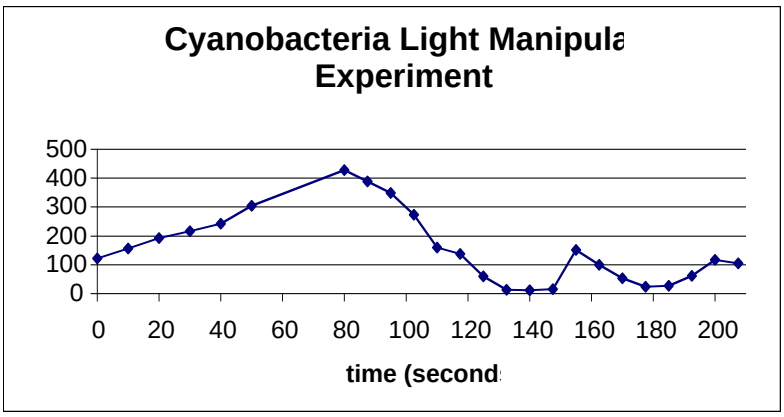

Figure 3.20: Light manipulation experiment in which each peak represents when the shade was removed from the mat. At 0 seconds the mat was covered, at 80 seconds the mat was in direct sunlight, at 140 seconds the mat was covered again, and at 160 seconds the mat was in direct sunlight.

3.2.6.2 Purple Sulfur Bacteria

Purple sulfur bacteria mats were studied upstream from the Cave Spring and Fissure Spring sites (figure 3.21). These mats formed in a shallow area off the shore of the river's small point bar. Purple sulfur bacteria are photosynthetic sulfur oxidizing bacteria similar to the green sulfur bacteria observed at Fissure Spring. This purple sulfur mat appeared to coexist with a green sulfur mat. The purple mat dominated shaded areas behind rocks and leaves, whereas the cyanobacteria mat was observed in areas of direct sunlight. In some areas, a layer of cyanobacteria existed underneath the buoyant purple sulfur bacteria. When the cyanobacteria and purple sulfur bacteria were collected together in a falcon tube the cyanobacteria settled at the bottom of the tube and the purples bacteria stratified to middle of the water column. This was similar to their position *in situ* (figure 3.21).

Figure 3.21: Pictures of the purple sulfur bacteria in the water and in the falcon tube.

By simply placing a shadow over the mats the purple sulfur bacteria were able to quickly adjust to changes in light by gliding vertically within the mat. When the shadow was removed and the light was directly hitting the mat the bacteria immediately disappeared into the sediment. A profile of the purple sulfur bacteria revealed the sulfide gradient associated with the bacteria (figure 3.22). Similar to the cyanobacteria, the sulfide concentrations decrease with depth within the purple sulfur mat. Unlike the cyanobacteria, the sulfide concentrations increase as a function of depth into the water underlying the mat. The profile shows that there is a sulfide gradient above and below the purple mat (figure 3.22). The buoyancy and motility of the sulfur bacteria allows them to exist between the two gradients.

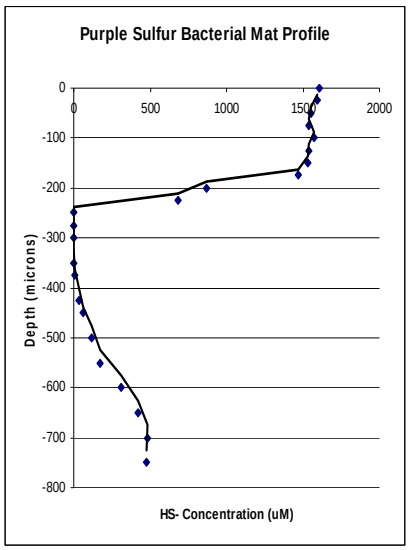

Figure 3.22: Profile of the purple sulfur bacteria mat showing a sulfide gradient from above and below.

4.0 Discussion

4.1 Elemental Sulfur Solubility

Elemental sulfur exists in solution in two forms: dissolved and colloidal. Through a series of experiments both forms were identified using voltammetry. The organic surfactant, SDS, used in the experiments enables one of the forms to be stabilized in solution, allowing it to be detected with the electrodes at a potential of -1.2V. In a solution of suspended elemental sulfur made from acidifying thiosulfate in cave spring water, the voltammetric scans show only one peak at -0.8V. When SDS was added to the solution, a second peak at -1.2V appears. Filtering the solution with a variety of filters gave evidence that the peak at -1.2V is dependent on the size of the sulfur particles in solution. Other techniques for dissolving the sulfur, adding the SDS, and filtering the solutions were investigated. The dependence on SDS for elemental sulfur solubility was consistent for all techniques. This dependence further supports the theory that the peak at -1.2V represents a form of sulfur solubilized by SDS. Filtration of sulfur/SDS solutions resulted in the disappearance of the peak at -1.2V in most cases suggesting that the

colloidal sulfur was filtered out of solution. The inconstancy with the disappearance of the sulfur peak at -1.2V upon filtration may represent variation in particle size. The variation in particle size may be controlled by the methods by which the sulfur was dissolved in solution.

In the Frasassi cave system elemental sulfur was detected in a variety of cave sites with a potential of -1.2V. It is known that sulfur-utilizing organisms will generate organic polymers, which are used by the organisms to store elemental sulfur intercellularly or extracellularly. SEM images taken by Dr. Jenn Macalady of a Cave Spring δ-proteobacteria samples showed intercellular sulfur globules (figure 4.1) and further support that organics surfactants produced by the sulfur bacteria at Frasassi will solubilize elemental sulfur. The Raman Spectroscopy results also give supporting evidence that elemental sulfur is stored by the Cave Spring biofilm.

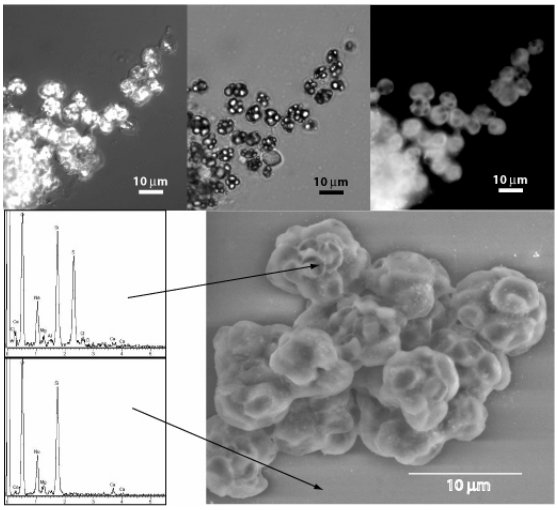

Figure 4.1: SEM image of δ-proteobacteria showing intercellular sulfur globules. (Dr. Jenn Macalady, Penn State University)

4.2 Microbial communities of the Frasassi cave system and their chemical niches

4.2.1 Feathery Biofilm

Although the white feathery biofilms found at Cave Spring, Pozzo di Cristali, and Ramo Sulfureo are unique to the specific chemistry of their environments, they are all characterized by the same physical and chemical features. These biofilms are refered to as "*thiothrix*-like" communities and are comprised mostly of δ-proteobacteria. The *thiothrix*-like mats are much thicker than other mats found in the caves, ranging in thickness from a few hundred microns to about a centimeter. These white mats thrive in flowing streams and attach to rocks for stability in the moving water.

Voltammetric measurements showed sharp sulfide gradients coupled with intermediate species of sulfur in association with these thicker mats. Elemental sulfur was also detected in the mats with voltammetry. The SEM image (figure 4.0) and Raman Spectroscopy results showed that elemental sulfur was stored by the microorganisms in this the white mat. It has been determined through voltammetry, SEM imaging, Raman Spectroscopy, and genetic analysis that the "thiothrix-like," white feathery biofilm mats in the Frasassi Cave System are storing elemental sulfur by solubilizing it with organic polymers.

4.2.2 Thin White Biofilm

In contrast to the thick "thiothrix-like" biofilms, thin biofilms existed in stagnant waters of the Frasassi caves. These thin biofilms were dominated either by *Beggiatoa spp* or *Thiovulum*. It was difficult to measure a detailed profile of these thin mats; however, the measurements of the water column provide information about their effects on the chemistry. Sharp gradients were not seen with *Beggiatoa spp* and *Thiovulum*

mats. Instead sulfur chemistry of the mats and associated water columns were constant with depth. This homogenous nature is expected for *Thiovulum* mats. *Thiovulum* mats will create a veil. This veil enabled these mats to mix the waters, cycling H_2S evenly through the system.

4.2.3 Phototrophic Biofilm

Photosynthesis has shown to be significant to sulfide oxidation outside of the cave environment. The light manipulation experiments conducted *in situ* showed the quick response time of the cyanobacteria mats and suggested that the rate of sulfide oxidation was dependent on photosynthesis.

The purple sulfur bacteria were sensitive to the amount of sunlight and physically moved to adapt to changes in light intensity. Voltammetric measurements of the purple sulfur bacteria mat over time and space gave evidence that the bacteria occupy a narrow chemical niche, in the interface between an overlying and underlying sulfide gradient (figure 3.26). Their motility feature also allowed them to quickly adapt to shifts in the position of this gradient, as well as to light intensity.

The intermediate chemistry associated with the phototrophic mats, their sharp vertical sulfide gradient, and the light manipulation experiment indicated that the rate of sulfide oxidation was faster than abiotic rates. Although the rates were not calculated, it was obvious that photosynthesis drives sulfide oxidation. Unlike most cyanobacteria, the cyanobacteria studied at Frasassi used H_2S as an electron donor instead of H_2O.

4.3 Defining chemical niches based on intermediate sulfur chemistry

The intermediate sulfur chemistry measured throughout a number of microbial communities was found to be a function of the dominant species of bacteria, time, space, and minor environmental fluctuations. Figure 4.1 compares the intermediate chemistry measured in a beggiatioa mat, δ-proteobacteria mat, and *Thiovulum* mat studied at various cave sites. From this comparison, it can be inferred that different microbial communities will oxidize sulfide through different pathways producing different intermediates. For example, the δ-proteobacteria (shown in blue) oxidized sulfide to elemental sulfur and polysulfide; the *Thiovulum* mat (shown in red) oxidized sulfide to elemental sulfur and thiosulfate. Also, the metabolism of these microbes was not limited to sulfide. Elemental sulfur, polysulfide, and thiosulfate can be directly oxidized to obtain energy.

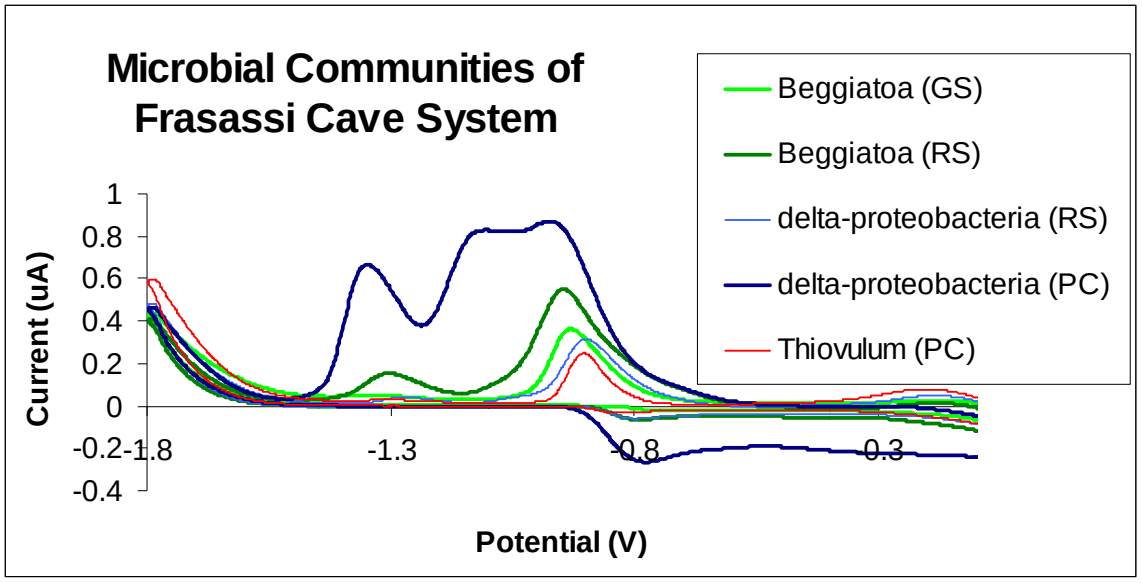

Figure 4.2: Voltammetric scans at CV 1 V/s summarizing the chemistry of microbial communities in the Frasassi cave system. These scans were taken in 2005.

The rate of sulfide oxidation can be infered by the intermediate chemistry as a function of the type of sulfur compounds present and the rate at which they change over time and space. As seen with vertical profiles, intermediates such as polysulfide and elemental sulfur are often measured well into the mat and change in concentration with depth. The presence of intermediate sulfur compounds *in situ* implies that sulfide oxidation is the dominant process in the environment.

The intermediate sulfur chemistry measured at Pozzo di Cristali in 2005 and 2006 suggests a difference in the redox conditions between the two years. The intermediate species of sulfur present in 2005 are evidence that the rate of sulfide oxidation was much faster in 2005. In addition, the data showed that sulfide concentrations decreased with progressive measurements downstream. In 2006, only sulfide was measured in the biofilms and the sulfide concentrations increased with progressive measurements downstream. The shift in sulfur chemistry between 2005 and 2006 can be attributed to the observed change in groundwater level. The water level in Pozzo di Cristali was higher in 2006, which created conditions favorable to sulfur reduction. High groundwater levels may have been too deep in 2006 for oxygen to penetrate far enough to form a sulfide oxidation gradient. The ecosystem studied at Pozzo di Cristali provided a great example for how microbial communities can shift their function to accommodate changes in the environment.

4.4 Rates of sulfide oxidation and its significance to cave formation: Pozzo di Cristali

Canfield et al. (2005) presented biotic rates which were much faster than abiotic rates in thiothrix mats V'_{max} values above 1.5×10^{-8} M h^{-1}. The V'_{max} value used for the biotic rate calculations was 1.5×10^{-3} M h^{-1}, implying that the rate should be 9×10^{-4} M h^{-1}. These conditions, however, assume that the concentration of H_2S and O_2 are the same. This is not the case in the Frasassi Caves, specifically at the cave site Pozzo di Cristali.

The rate of sulfide oxidation measured in the field showed that sulfide oxidation was occurring much faster than the abiotic rate predicted by equation 1.19. It was also calculated that the predicted biotic sulfide oxidation was slower than abiotic rate, which was not expected. It is important to keep in mind that many assumptions and estimations were applied to the rate equations, yielding rough estimates of rate values. However, the rate data collected can provide a general understanding of the order of oxidation rates and, furthermore, suggest controls on the rates.

Several factors contributed to the error in calculating oxidation rate. The equations did not consider intermediate species of sulfur, either as a product or as an oxidation source. Zhang and Millero (1994) suggested that the rate of oxidation is significantly influenced by the intermediate chemistry. Although equations provide by Zhang and Millero (1994) represent rates based on intermediate chemistry, it was difficult to measure intermediate species of sulfur and, therefore, the equations were not used.

Data specific to thiothrix was used to representing δ-proteobacteria at Pozzo di Cristali for calculating oxidation rates. Several assumptions were made in addition to

classifying the δ-proteobacteria mat as thiothrix for calculation purposes. Data provided for $K_{m\text{-}H2S}$ by Canfield et al (2005) was given as a range between 2.4 and 12.2 x 10^{-6}M, from which the average was derived and used. Also, the numbers for $K_{m\text{-}H2S}$ and $K_{m\text{-}O2}$ were representative of a thiothrix mat with a cell density of 10^7. It was estimated that the cell density of the δ-proteobacteria mat was 10^9. In addition to the K and V_{max} values, all values taken from Canfield et al. (2005) were representative of conditions of equal concentrations of [H_2S] and [O_2].

A significant factor to consider when interpreting the rate calculations is that all oxidation rate calculations only used O_2 as an electron acceptor. Nitrate can also be used, and from the lack of oxygen in the cave's sub-environments, nitrate is suggested to be important to the oxidation of sulfide.

Although gypsum was not observed at the Cave Spring site, gas measurements indicated that hydrogen sulfide was being released into the atmosphere. In the sheltered cave environments, such as at Potto di Cristali, sulfide was oxidized on the walls and reacted with the calcium from the limestone to form gypsum. Hydrogen sulfide degassing from the aqueous regions provides the sources of sulfur for gypsum formation. The rate of H_2S diffusion may have implications for the rate at which H_2S is being supplied to the walls and ceilings. This may affect the rate at which sulfide is oxidized and the rate at which sulfuric acid is produced.

5.0 Conclusion

Microbial communities of the Frasassi cave system, Italy are biologically mediating sulfuric acid speleogenesis by catalyzing sulfur oxidation reactions. As sulfidic waters feed the karst system, sulfur-oxidizing bacteria, dominated by δ-proteobacteria, *Beggiatoa spp*, and *Thiovulum*, are catalyzing the oxidation of the sulfide. Voltammetry was proven to be a powerful tool for measuring the *in situ*, real-time chemistry in the sub-aqueous ecosystems of the Frasassi caves. The Au/Hg amalgam glass electrodes were able to measure changes in sulfur chemistry over sub-millimeter intervals. The intermediate sulfur chemistry detected for each microbial community describes the rate of sulfide oxidation, the pathways by which sulfide is oxidized, and the chemical niches that select for different species of sulfur bacteria. Changes in the sulfur chemistry over time and space were found to be a function of changes in environmental conditions. The chemical variation also reflected shifts in the microbial communities to adapt the environmental changes, showing that the chemical and biological systems are closely linked.

The subaqueous ecosystems of the Frasassi cave system demonstrate the significance of the relationship between biology, chemistry, and the environment. Biotic processes considerably influence the pathways through which sulfur is oxidized, the intermediate sulfur species produced, and the rate at which these reactions happen. Understanding chemical cycling through these simple aqueous environments can be applied to the investigation of sulfuric acid speleogenesis as well as to more complex environments.

6.0 Future Work

Upon the completion of this thesis many questions have developed in relation to distinguishing voltammetric signals of polysulfide, sulfide, and elemental sulfur. Further research is needed to understand the size range of colloidal sulfur, the affects of filtration on the solutions made, the significance of organic and inorganic complexes to colloidal sulfur particles, and the distinction between colloidal and dissolved sulfur using voltammetry.

We have assumed for this thesis that the peak observed at -0.9V represented sulfide and the peak at -0.7V represented polysulfide. When sulfide and polysulfide coexist in solution only one peak is detected, indicating that the electrodes may not be able to distinguish between the two. At higher concentration of sulfide or polysulfide the situation becomes further complicated, as three peaks are often seen. The task of distinguishing between the three peaks and the difference between polysulfide and sulfide has not been explored in detail. Further research is needed to identify each of the three peaks, as well as to identify both sulfide and polysulfide in sulfidic environments.

Further research is also needed to determine the rate of sulfide oxidation in the caves. The comparison between the *in situ* rate of sulfide oxidation and the predicted rates suggests that sulfide oxidation *in situ* is much faster. A number of factors could contribute to the *in situ* rate, including oxygen and nitrate concentrations, the intermediate chemistry, changes in flow rate, degassing, and microbial species composition. Further investigation would be needed to understand the *in situ* controls on sulfide oxidation.

Literature Cited

Amend, J.P., Rogers, K.L., Shock, E.L., Gurrieri, S., and Inguaggiato, S. (2003) Energetics of chemolithoautotrophy in the hydrothermal system of Vulcano Island, southern Italy. *Geobiology*, 1, 37-58.

Canfield, D. E., Thamdrup, B., & Kristensen, E. (2005) *Aquatic Geomicrobiology.* Boston: Elsevier.

Chen, K.Y., & Morris, J. C. (1972). Kinetics of Oxidation of Aqueous Sulfide by O_2. *Environmental Science and Technology,* 6 (6), 529-537.

Hagen, K. D., and Nelson, D. C. (1997). Use of Reduced Sulfur Compounds by *Beggiatoa spp Spp*: Enzymology and Physiology of Marine and Freshwater Strains in Homogeneous and Gradient Cultures. *Applied and Environmental Microbiology*, 63 (10).

Kamp, A., Stief, P., and Schulz-Vogt, H. N. (2006). Anaerobic Sulfide Oxidation with Nitrate by a Freshwater *Beggiatoa spp* Enrichment Culture. *Applied and Environmental Microbiology*, 72 (7).

Kleinjan, W.E., Marcelis, C.L.M, Keizer, A, Janssen, A.J.H, & Stuart, M.A.C. (2006) Foam formation in a biotechnological process for the removal of hydrogen sulfide from gas streams. *Colloids and Surfaces A: Physicochem. Eng. Aspects,* 275, 36-44.

Kleinjan, W.E., Keizer, A., & Janssen, A.J.H. (2005) Kinetics of the Reaction between Dissolved Sodium Sulfide and Biologically Produced Sulfur. *Ind. Eng. Chem. Res.,* 44, 309-317.

Kleinjan, W.E., Keizer, A., Janssen, A.J.H. (2005) Equilibrium of the reaction between dissolved sodium sulfide and biologically produced sulfur. *Colloids and Surfaces B: Biointerfaces*, 42, 228-237.

Kleinjan, W.E., Keiser, A., & Janssen, A.J.H. (2003) Biologically Produced Sulfur. *Top Current Chemistry*, 230, 167-188.

Knickerbocker, C, Nordstrom, D.K., & Southam, G. (2000) The role of 'blebbing' in overcoming the hydrophobic barrier during biooxidation of elemental sulfur by thiobacillus thiooxidans. *Chemical Geology,* 169, 425-433.

Langmuir, Donald. (1997) *Aqueous Environmental Geochemistry*. New Jersey: Prentice Hall.

Lorenson, G. (2006) Application of *in situ* Au-amalgam microelectrodes in Yellowstone National Park to guide microbial sampling: an investigation into arsenite and polysulfide detection to define microbial habitats. M.S. Thesis, University of Vermont, 1-176.

Montanari, A., Galdenzi, S, & Rossetti G. (2002). *Drops of Time: Strolling among the stones.* Ancona, Italy: Aniballi Grafiche

O'Brien, D. J. & Birkner, F.B. (1977). Kinetics of Oxygenation of Reduced Sulfur Species in Aqueous Solution. *Environmental Science and Technology*, 11 (12), 1114-1120.

Macalady, J. L., Lyon, E., Koffman, B., Galdenzi, S., and Mariani, S. (2006). Dominant microbial populations in limestone-corroding stream biofilms, Frasassi cave system, Italy. *Applied and Environmental Microbology*, 72 (8).

Madigan, M.T., Martinko, J.M., & Parker, J. (2002) Brock Biology of Microorganisms, 10. New Jersey: Prentice Hall.

Rosen, E. and Tegman, R., 1971, A Preparative and X-ray Powder Diffraction Study of the Polysulfides Na_2S_2, Na_2S_4, and Na_2S_5: Acta Chemica Scandinavica, v. 25: p. 3329-3336.

Steudel, R. & Holdt, G. (1988) Solubilization of Elemental Sulfur in Water by Carionic and Anionic Surfactants. *Angew. Chem. Int. Ed. Engl,* 27 (10), 1358-1359.

Steudel, R, Holdt, G, & Naorka, G. (1986) "On the Autoxidation of Aqueous Sodium Polysulfide. Z Naturforsch B, 41, 1519-1522

Teske, A., & Nelson, D. C. (2006) The Genera *Beggiatoa spp* and Thioploca. Retrieved November 20, 2006, from file:///Volumes/homes/chaprender/jsp/showchap.jsp?chapnum=432

Vlasceanu, L., Sarbu, S.M., Engel, A.S., & Kinkle, B.K. (2000) Acidic Cave-Wall Biofilms Located in the Frasassi Gorge, Italy. *Geomicrobiology Journal,* 17, 125-139.

Williamson, M.A. and Rimstidt, J.D. (1992) Correlation between structure and thermodynamic properties of aqueous sulfur species: *Geochimica et Cosmochimica Acta*, 56, 3867-3880.

Zhang, J. Z., & Millero, F. J. (1994) Kinetics of Oxidation of Hydrogen Sulfide in Natural Waters. *American Chemical Society*, 26, 393-409.

Wang, F., Tessier, A., & Buffle, J (1998) Voltammetric determination of elemental sulfur in pore waters. *Limol. Oceanogr.*, 43(6), 1353-1361.